

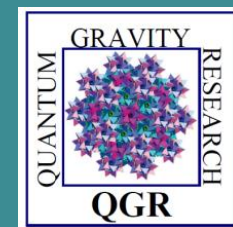
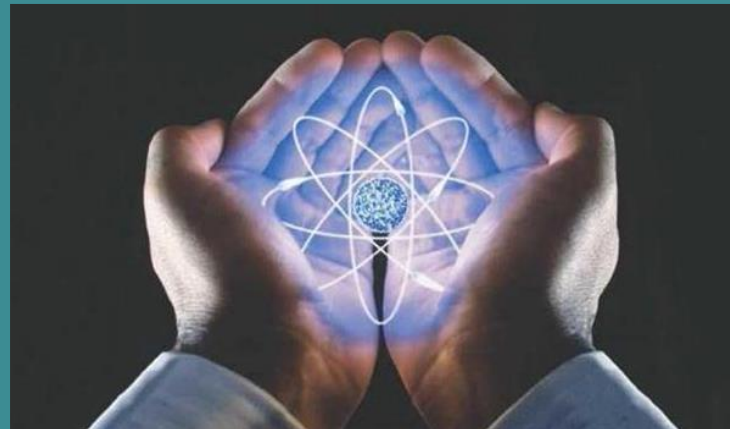
# Chemical and nuclear catalysis mediated by the energy localization in crystals and quasicrystals

Vladimir Dubinko<sup>1,3</sup>, Denis Laptev<sup>2,3</sup>, Klee Irwin<sup>3</sup>

<sup>1</sup>NSC Kharkov Institute of Physics & Technology, Ukraine

<sup>2</sup>B. Verkin Institute for Low Temperature Physics and Engineering, Ukraine

<sup>3</sup>Quantum gravity research, Los Angeles, USA



# Coauthors

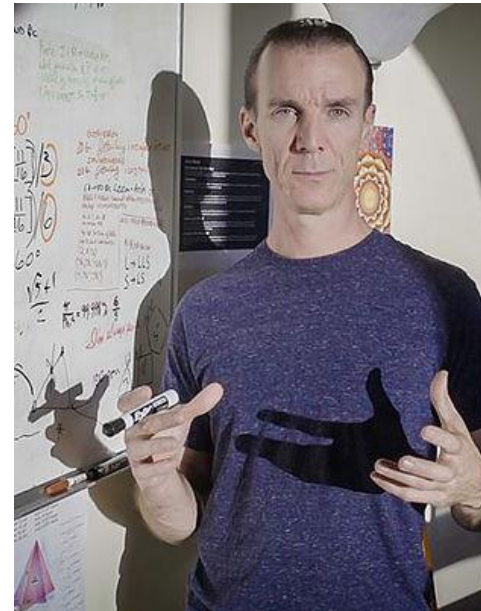
**Denis Laptev,**

B. Verkin Institute for Low Temperature Physics and Engineering,  
Ukraine



**Klee Irwin,**

Quantum Gravity Research,  
Los Angeles, USA



# Outline

- Localized Anharmonic Vibrations: history and the state of the art
- LAV role in **chemical** and **nuclear** catalysis
- MD simulations in crystals and quasicrystalline clusters

# Energy localization in anharmonic lattices

In the summer of 1953 [Enrico Fermi](#), [John Pasta](#), [Stanislaw Ulam](#), and [Mary Tsingou](#) conducted numerical experiments (i.e. computer simulations) of a vibrating string that included a non-linear term (quadratic in one test, cubic in another, and a piecewise linear approximation to a cubic in a third). They found that the behavior of the system was quite different from what intuition would have led them to expect. Fermi thought that after many iterations, the system would exhibit [thermalization](#), an ergodic behavior in which the influence of the initial modes of vibration fade and the system becomes more or less random with [all modes excited more or less equally](#). Instead, the system exhibited a very complicated quasi-periodic behavior. They published their results in a [Los Alamos](#) technical report in 1955.

The **FPU paradox** was important both in showing the **complexity of nonlinear system** behavior and the value of computer simulation in analyzing systems.

# Localized Anharmonic Vibrations (LAVs)

A. Ovchinnikov (1969)

## Two coupled anharmonic oscillators

$$\ddot{x}_1 + \omega_0^2 x_1 + \varepsilon \lambda x_1^3 = \varepsilon \beta x_2$$

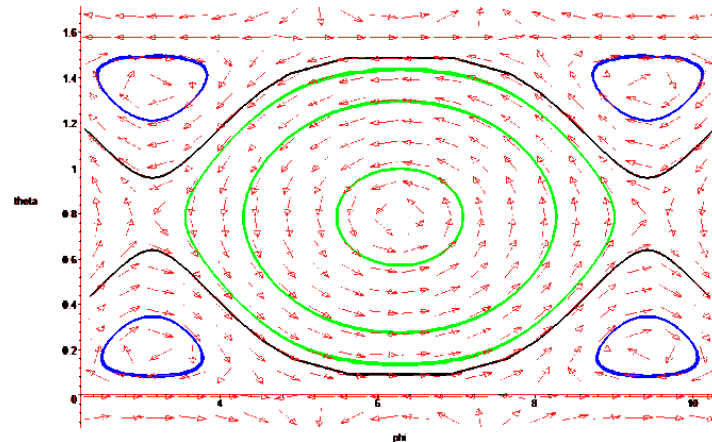
$$\ddot{x}_2 + \omega_0^2 x_2 + \varepsilon \lambda x_2^3 = \varepsilon \beta x_1$$

$$\tau = \frac{\omega_0}{\varepsilon \beta} \int_0^{\pi/2} \frac{d\eta}{\sqrt{1 - \left(\frac{3A_0\lambda}{4\beta}\right)^2 \sin^2 \eta}}$$

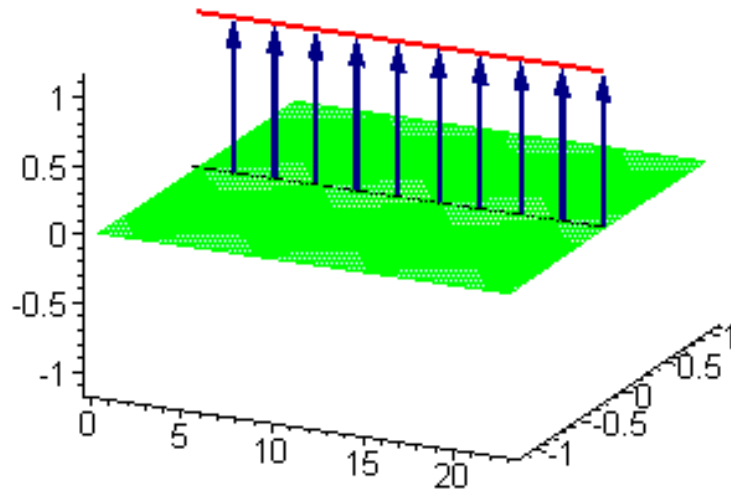
## Localization condition

$$A_0 > \frac{4\beta}{3\lambda} \Rightarrow \tau \rightarrow \infty$$

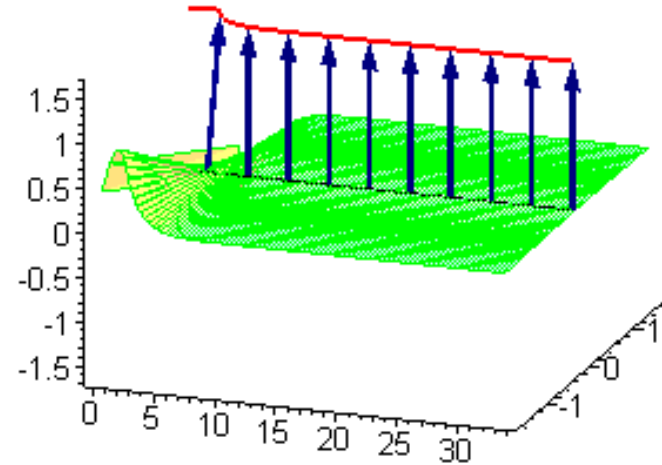
## Phase diagram



# Discrete Breathers

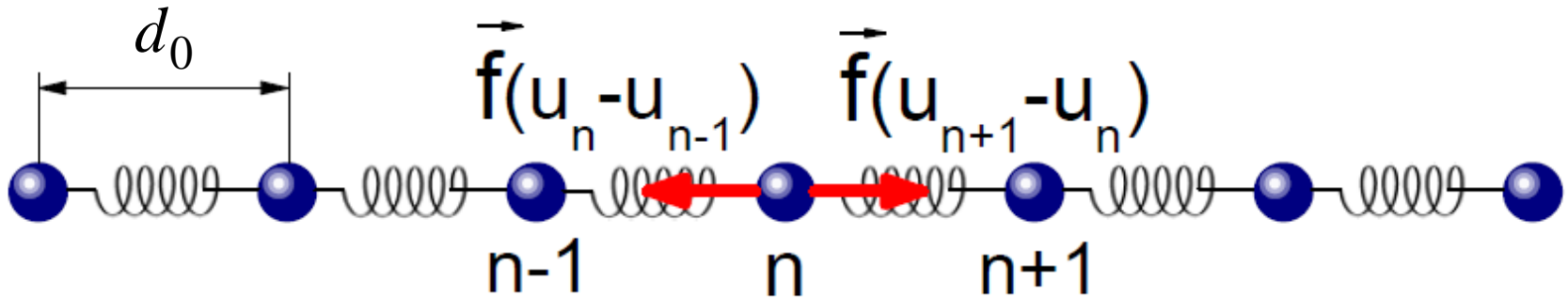


Sine-Gordon standing breather is a swinging in time coupled kink-antikink 2-soliton solution.



Large amplitude moving sine-Gordon breather.

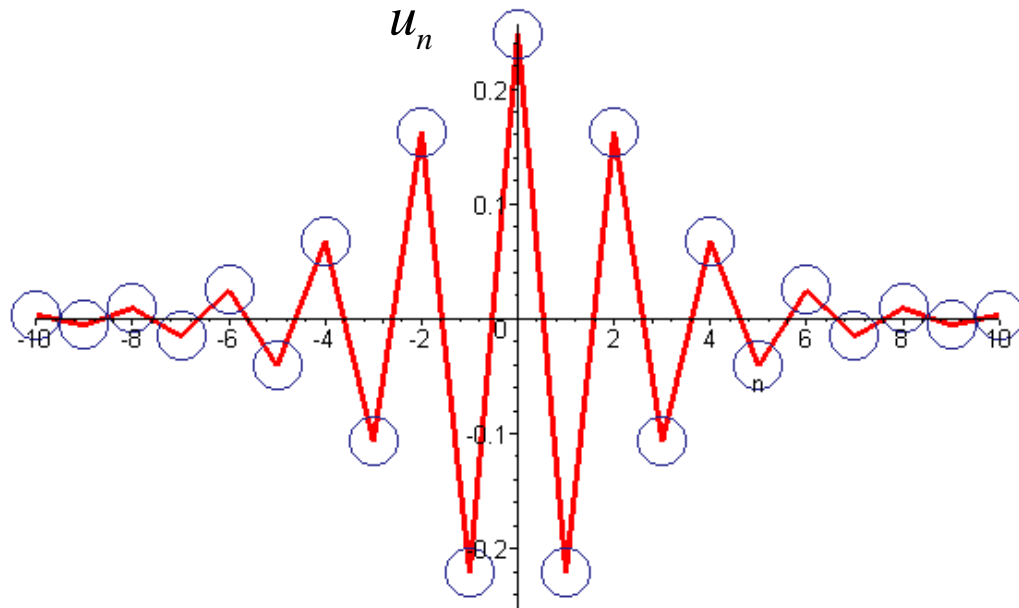
# 1D crystal — Hirota lattice model (nonlinear telegraph equations, 1973)



Equation of motion of Hirota lattice

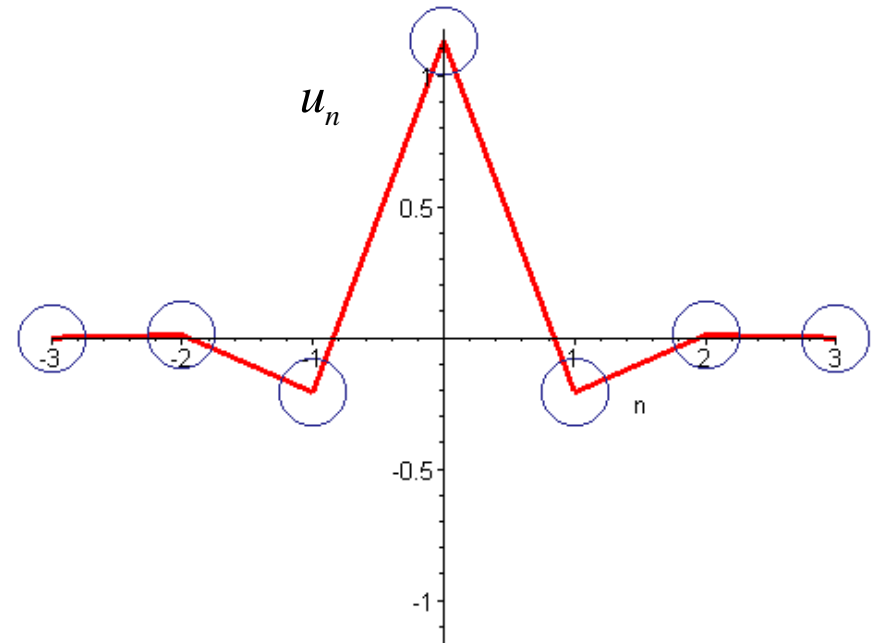
$$\frac{m\ddot{u}_n}{1 + \frac{\pi^2 \dot{u}_n^2}{4s^2}} = \frac{2}{\pi} \gamma d_0 \left\{ \operatorname{tg} \left[ \frac{\pi}{2} \left( \frac{u_{n-1} - u_n}{d_0} \right) \right] - \operatorname{tg} \left[ \frac{\pi}{2} \left( \frac{u_n - u_{n+1}}{d_0} \right) \right] \right\}$$

$$H = \left( \frac{2}{\pi} \right)^2 ms^2 \sum_{n=-\infty}^{+\infty} \left\{ \frac{1}{2} \ln \left[ 1 + \operatorname{tg}^2 \left( \frac{\pi p_n}{2ms} \right) \right] + \frac{1}{2} \ln \left[ 1 + \operatorname{tg}^2 \left( \frac{\pi}{2d_0} (u_{n-1} - u_n) \right) \right] \right\}$$



Standing **weakly localized DB**

Bogdan, 2002

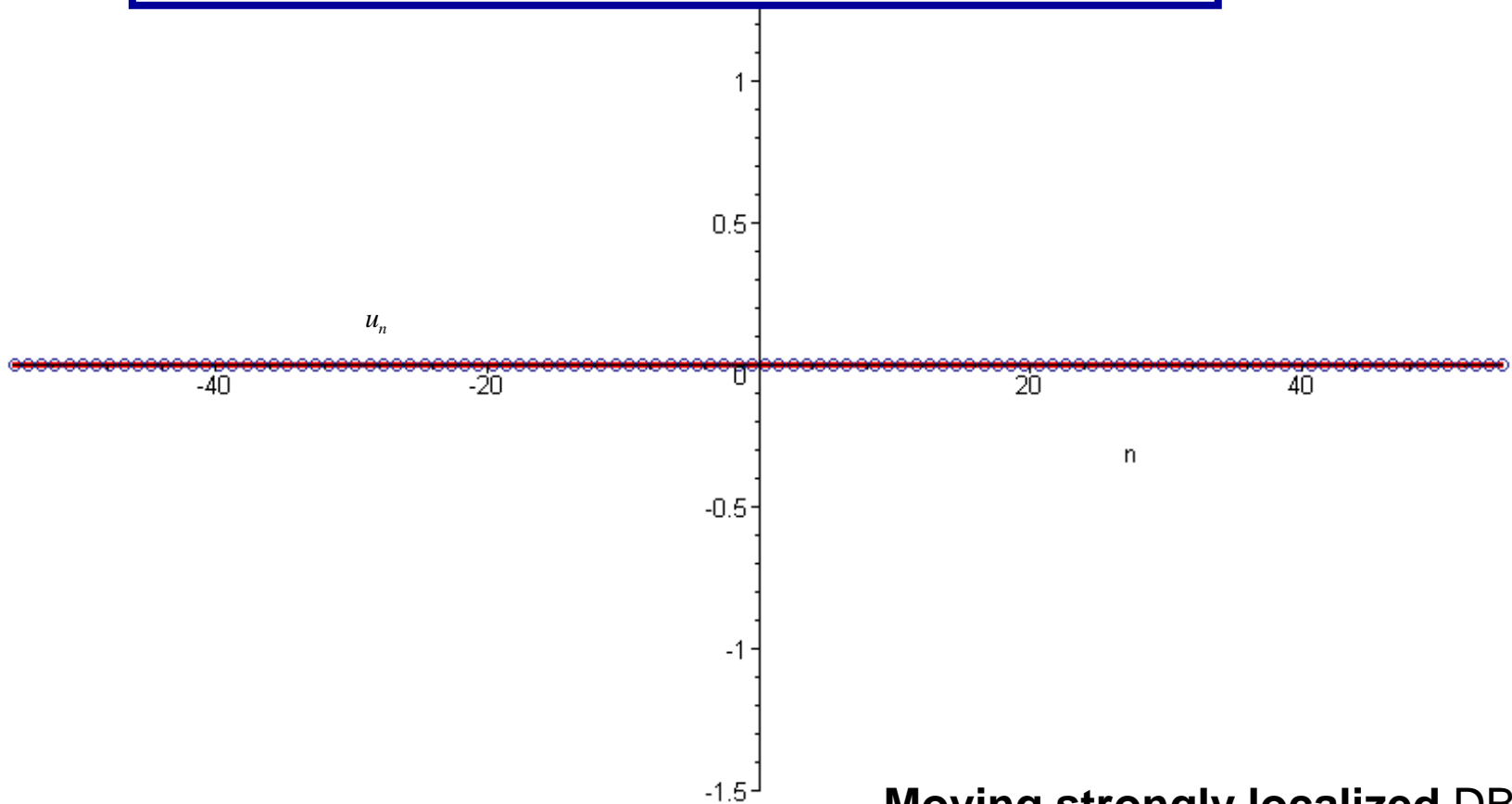


Standing **strongly localized DB**

$$u_n^{(b)} = \frac{2d_0}{\pi} \operatorname{arctg} \left[ \frac{\operatorname{sh}(\kappa d_0/2) \cos(knd_0 - \omega t)}{\sin(kd_0/2) \operatorname{ch} \kappa(nd_0 - Vt)} \right],$$

Bogdan, 2002

$$\omega = \frac{s}{d_0} 2 \operatorname{ch} \left( \frac{\kappa d_0}{2} \right) \sin \left( \frac{kd_0}{2} \right), \quad V = s \frac{\operatorname{sh}(\kappa d_0/2)}{\kappa d_0/2} \cos \left( \frac{kd_0}{2} \right).$$



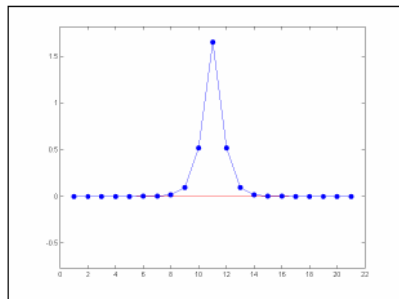
**Moving strongly localized DB**

## Nonlinear coupled oscillators



$$V = \sum V(X_n) + C W(X_n, X_{n+1})$$

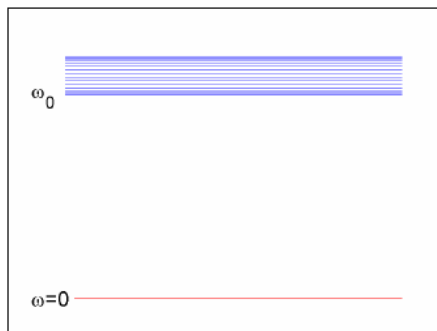
- Exact, periodic and localized solution



The concept of **LAV** in regular lattices is based on *large anharmonic* atomic oscillations in **Discrete Breathers** excited *outside the phonon bands*.

## Phonons

- Frequency band  $\omega_{ph}^2 = \omega_0^2 + 4C \sin^2 q/2$
- Non localized states

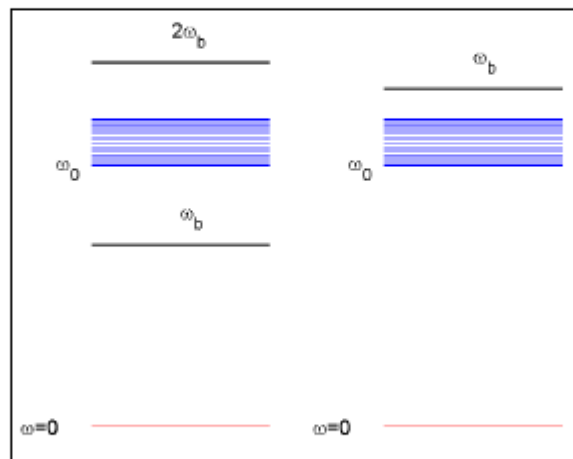


## Existence of breathers (1994)



Soft

Hard



$$\omega_b \notin [\omega_0, \omega_{f,\max}], \quad \omega_b'(E) \neq 0$$

# DBs in metals Hizhnyakov et al (2011)

PREDICTION OF HIGH-FREQUENCY INTRINSIC ...

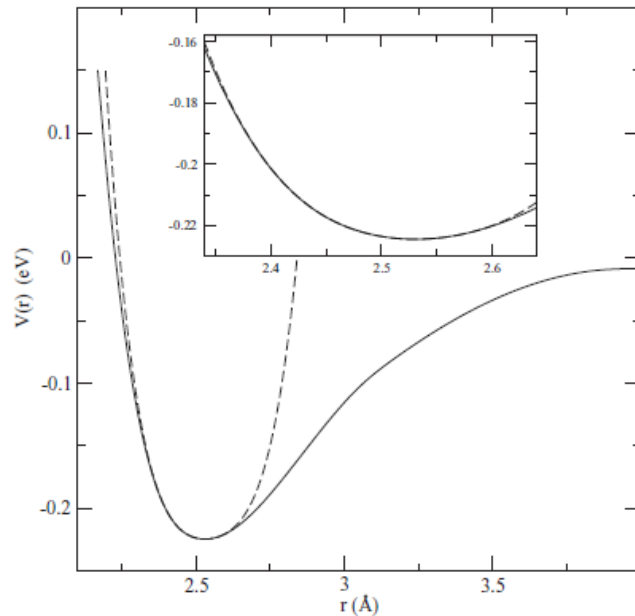


FIG. 1. The pair potential  $V(r)$  of Ni (solid line) and its approximation by the fourth-order polynomial (dashed line). The inset shows an expanded view.

The distance between the nearest atoms in Ni at room temperature is  $r_0 = 2.49$  Å and longitudinal sound velocity is  $v_l = 5266$  m/s. These values give  $\tilde{K}_2 = 2.75$  eV/Å<sup>2</sup> (as expected,  $\tilde{K}_2 > K_2$ ) and  $\tilde{\kappa} \approx 1.2$ . The distance  $r_0$  increases

HAAS, HIZHNYAKOV, SHELKAN, KLOPOV, AND SIEVERS

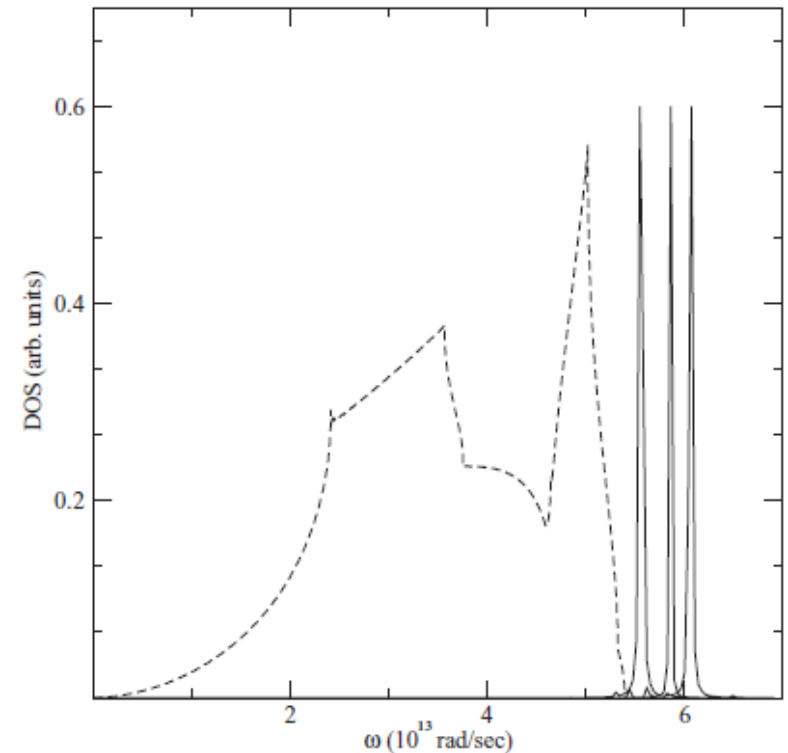
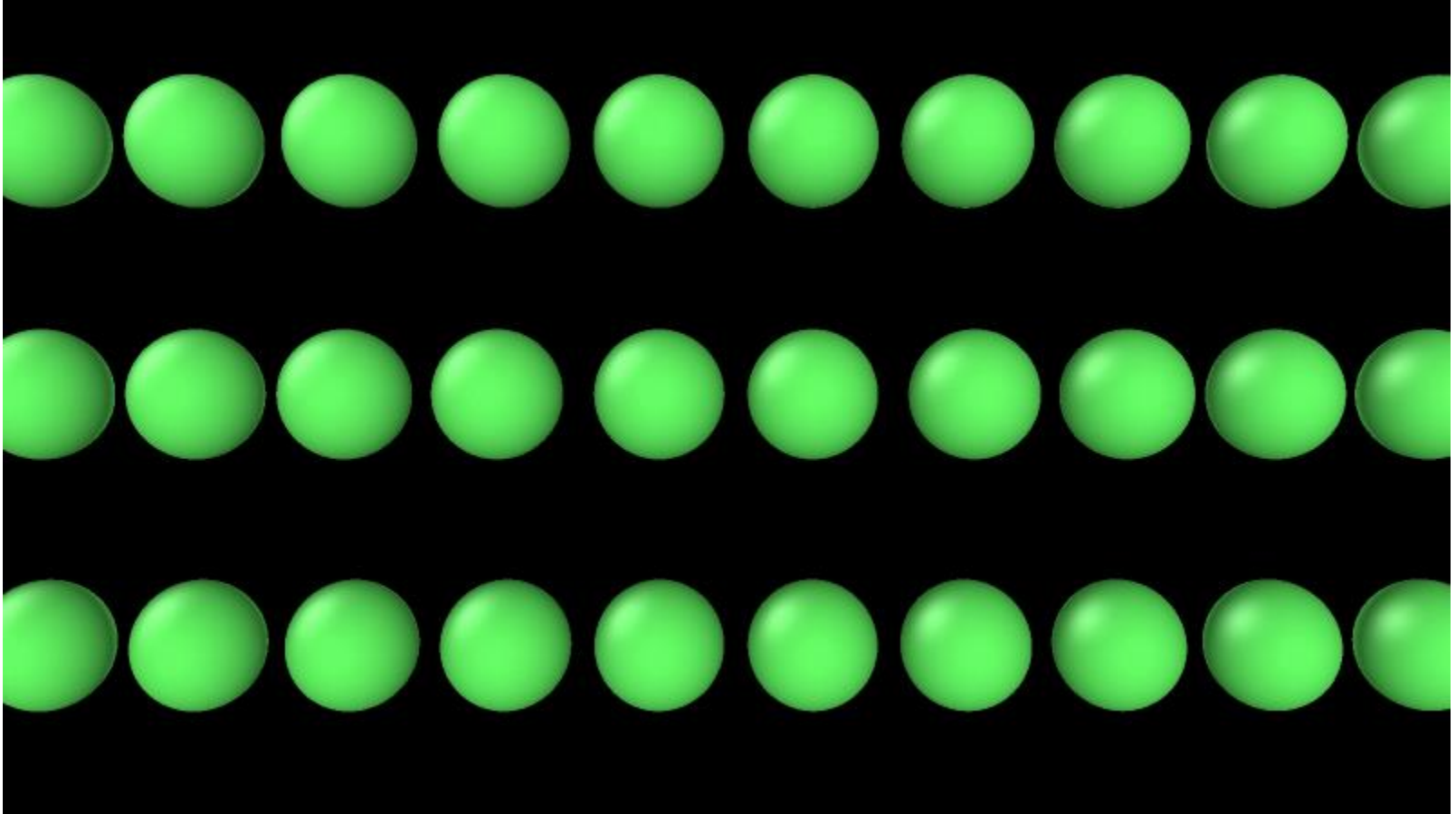
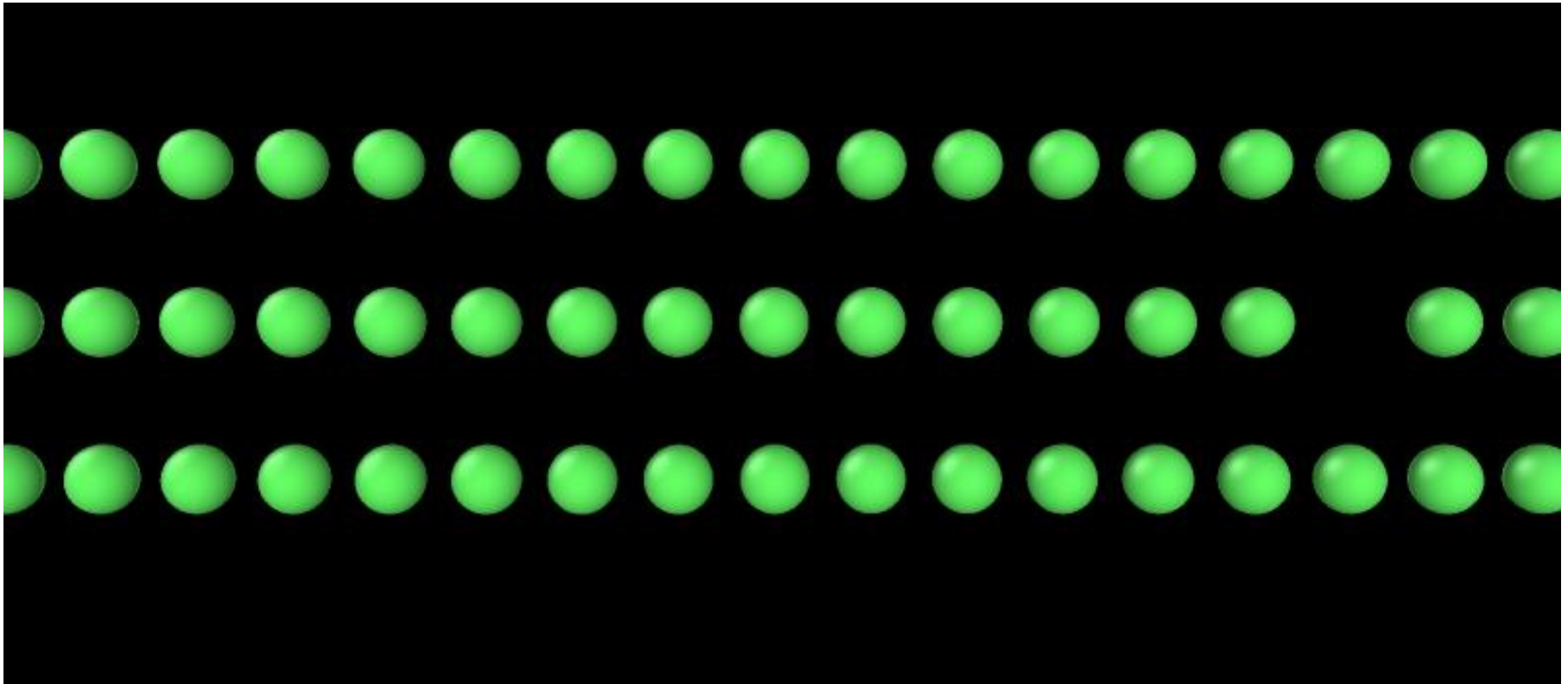


FIG. 2. Phonon density of states and three ILM spectral signatures for Ni. Phonon spectrum (dashed line) and spectrographs (solid line) of the different ILM's: The frequencies are 5.58, 5.86, and 6.07 ( $10^{13}$  rad/s) and the amplitudes of vibrations of the central bond are 0.18, 0.31, and 0.42 Å.

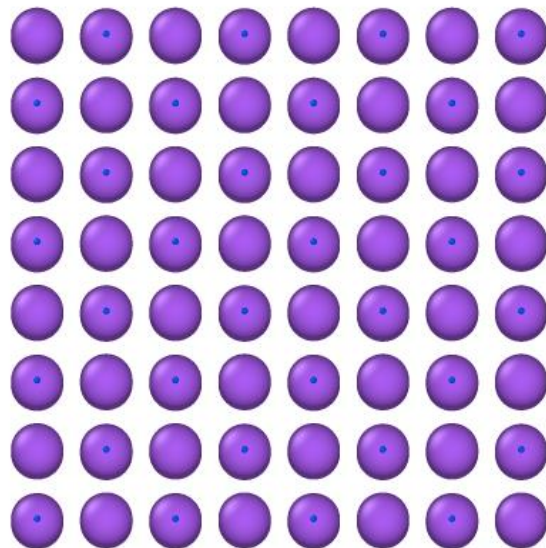
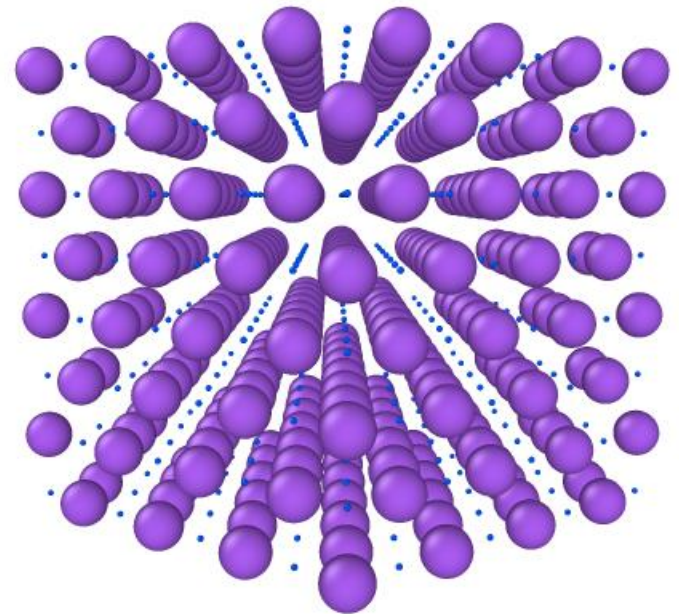
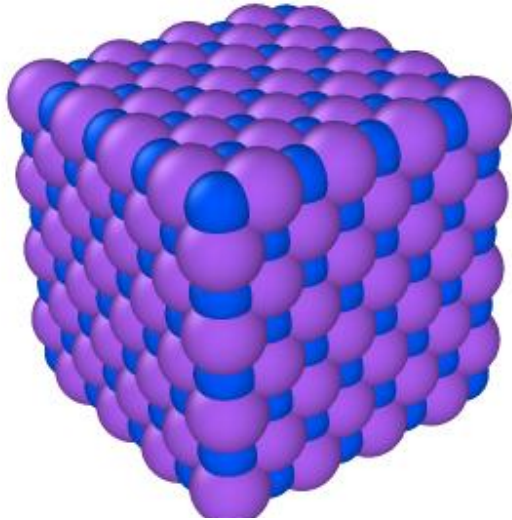
**Standing DB in bcc Fe:  $d_0=0.3 \text{ \AA}$**   
D.Terentyev, V. Dubinko, A. Dubinko (2013)



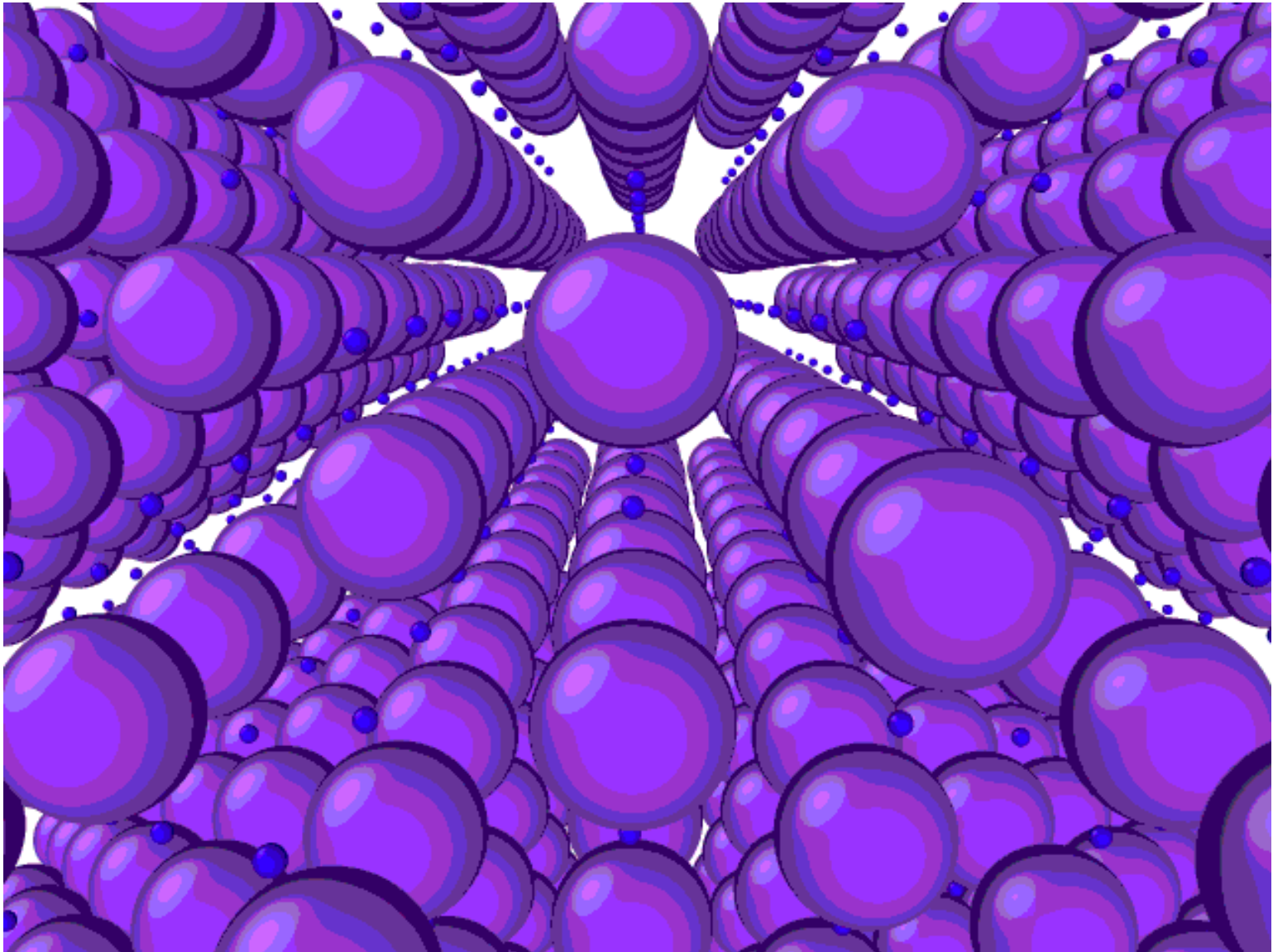
**Moving DB in bcc Fe:  $d_0=0.4 \text{ \AA}$ ,  $E=0.3 \text{ eV}$**   
D.Terentyev, V. Dubinko, A. Dubinko (2013)



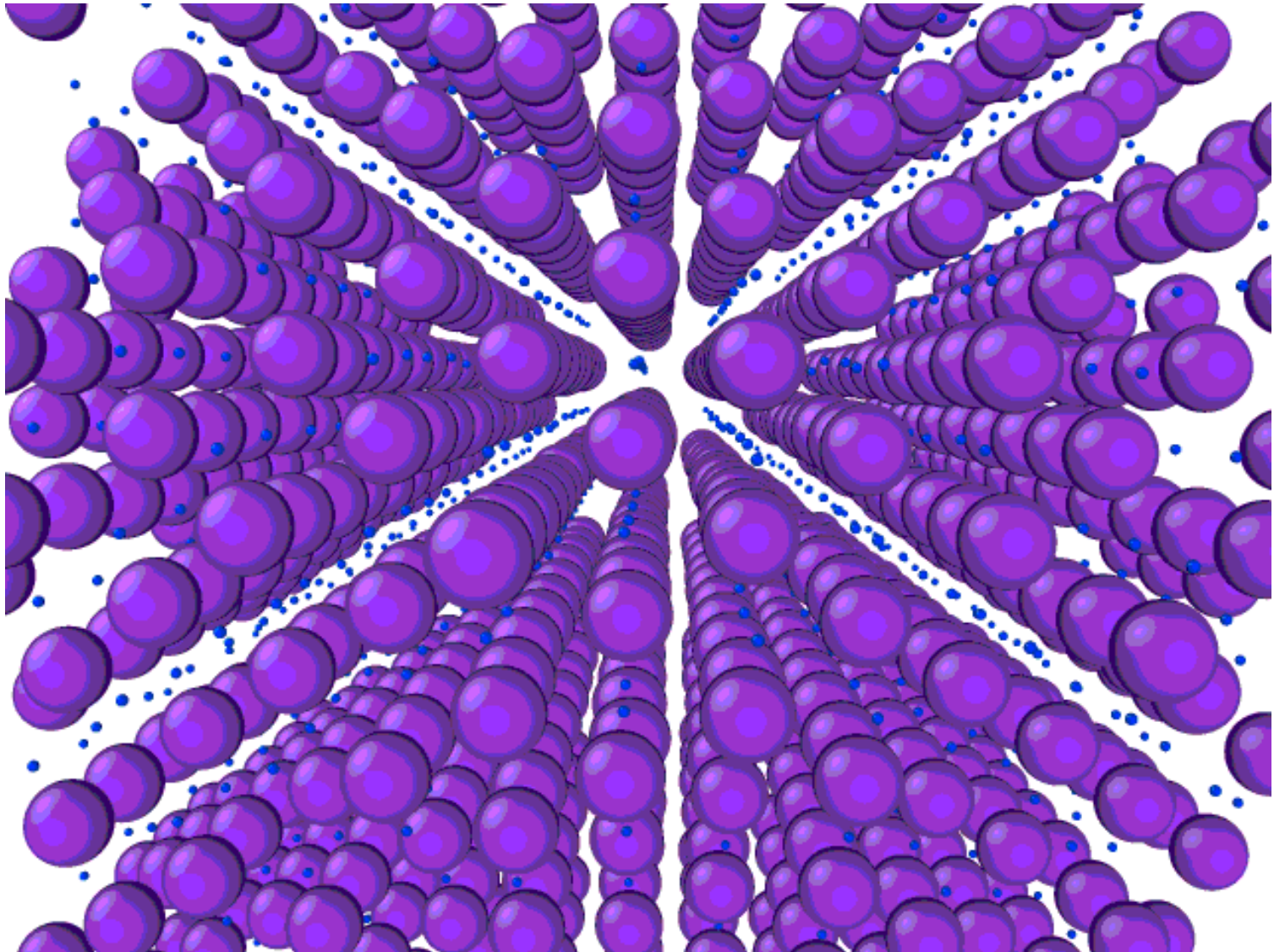
# Visualization of the PdH fcc Lattice (NaCl type)



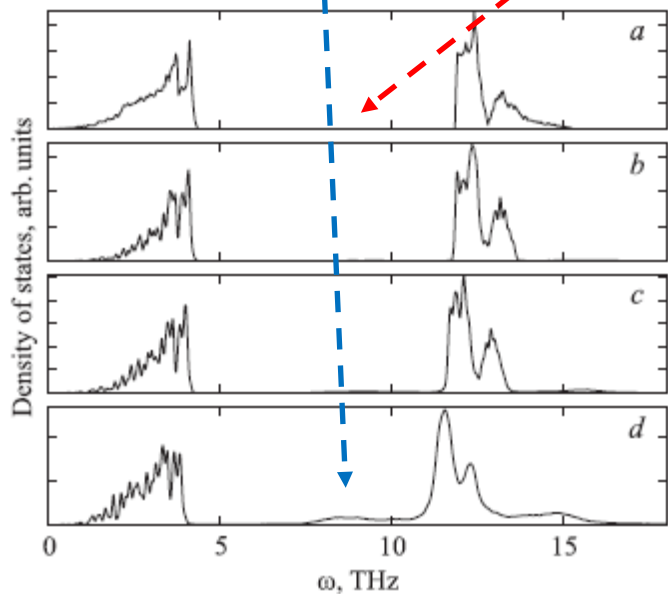
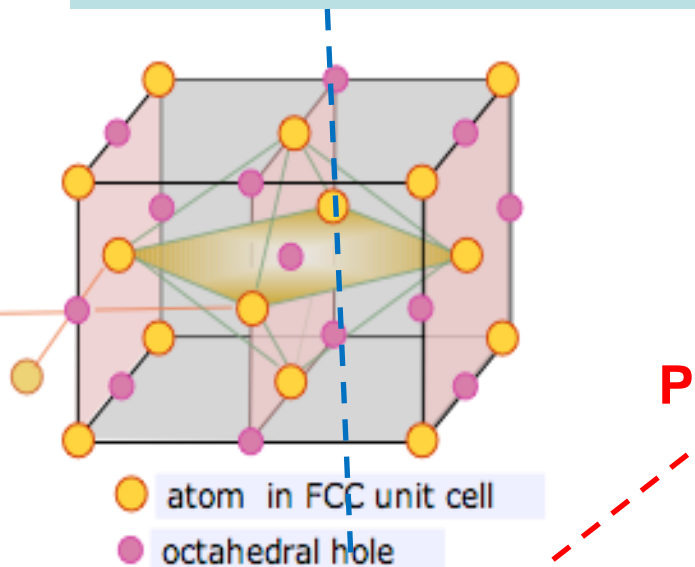
# Visualization of the PdH fcc Lattice Oscillations at $T=100$ K



# Visualization of the PdH fcc Lattice Oscillations at $T=1000\text{K}$

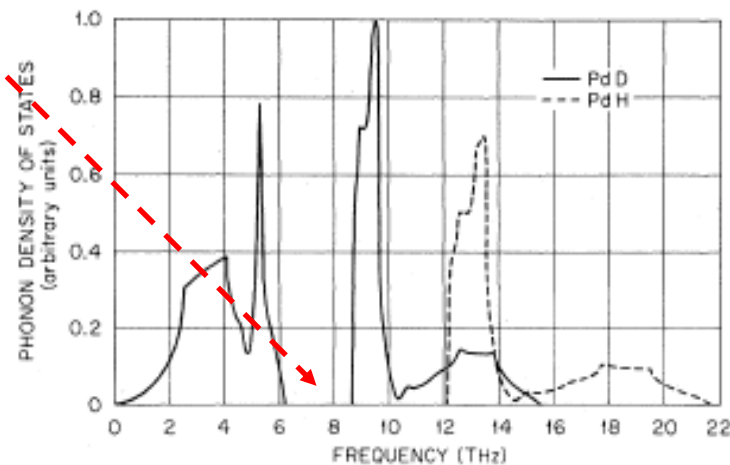
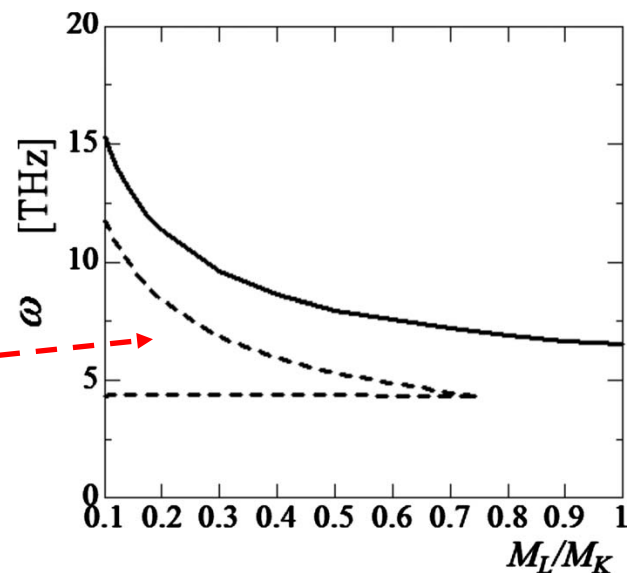


# Gap breathers in NaCl type lattices, Dmitriev et al (2010)



NaCl-type  $M_H/M_L = 10$  at temperatures  $T = (a) 0, (b) 155, (c) 310, \text{ and } (d) 620 \text{ K}$

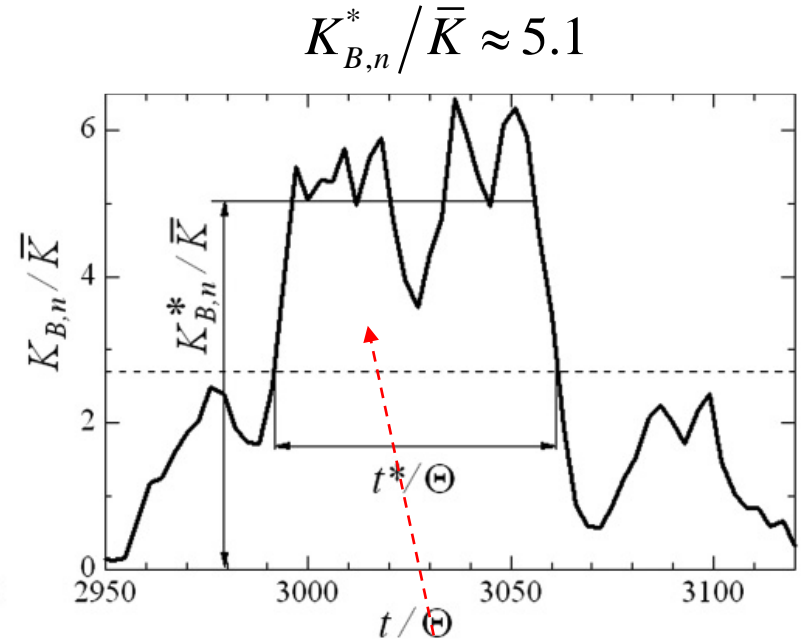
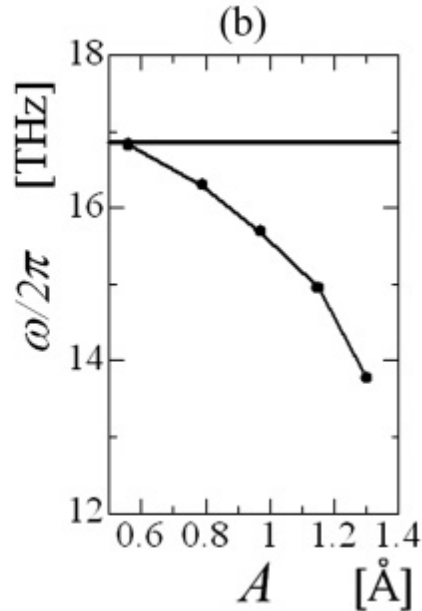
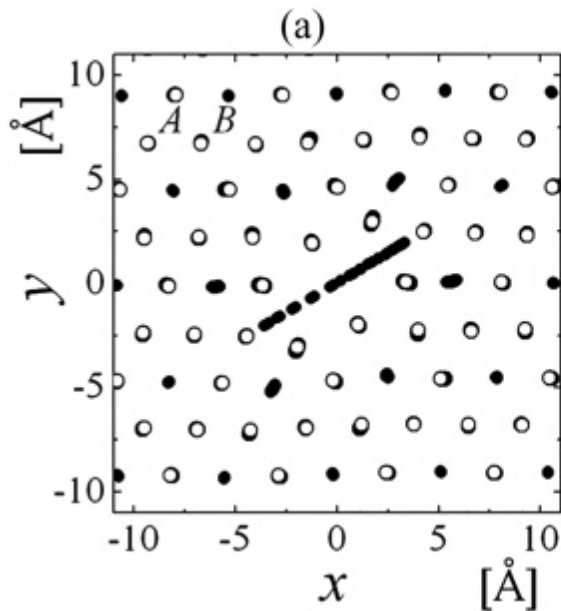
**Phonon Gap**



DOS for  $\text{PdD}_{0.63}$  and  $\text{PdH}_{0.63}$ ;  $M_H/M_L = 50; 100$   
 D pressure of 5 GPa and  $T = 600 \text{ K}$

# MD modeling of gap DBs in diatomic crystals at elevated temperatures

Hizhnyakov et al (2002), Dmitriev et al (2010)



$A_3B$  type crystals  $M_H / M_L = 10$

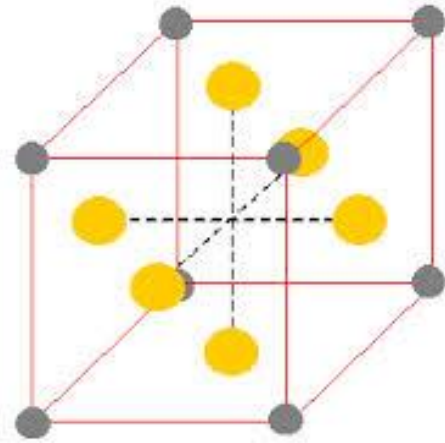
$t^*/\Theta \approx 70 \bar{K} = 0.1eV \geq 1000K$

In NaI and KI crystals Hizhnyakov et al has shown that DB amplitudes along  $\langle 111 \rangle$  directions can be as high as  $1 \text{ \AA}$ , and  $t^*/\Theta \sim 10^4$

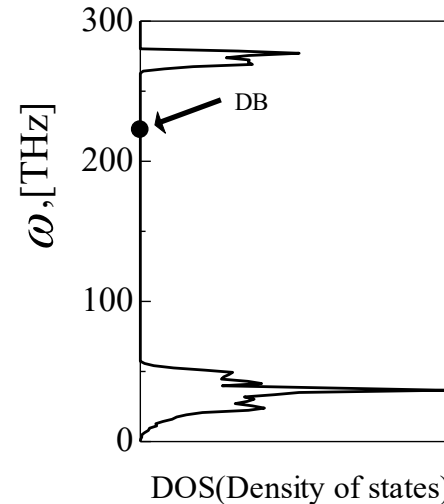
Lifetime and concentration of **high-energy light atoms** increase exponentially with increasing T

# MD modeling of gap DBs in diatomic crystals at elevated temperatures

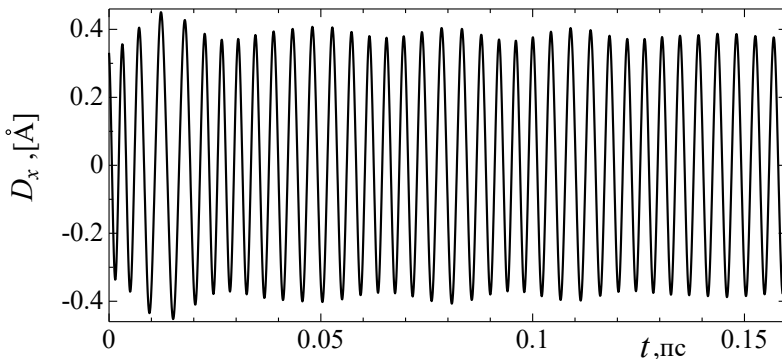
$A_3B$  type crystals, Kistanov, Dmitriev (2014),



$A_3B$  compound based on fcc lattice with Morse interatomic potentials. Grey atoms are **50 times lighter** than yellow (similar to the PdD crystal).

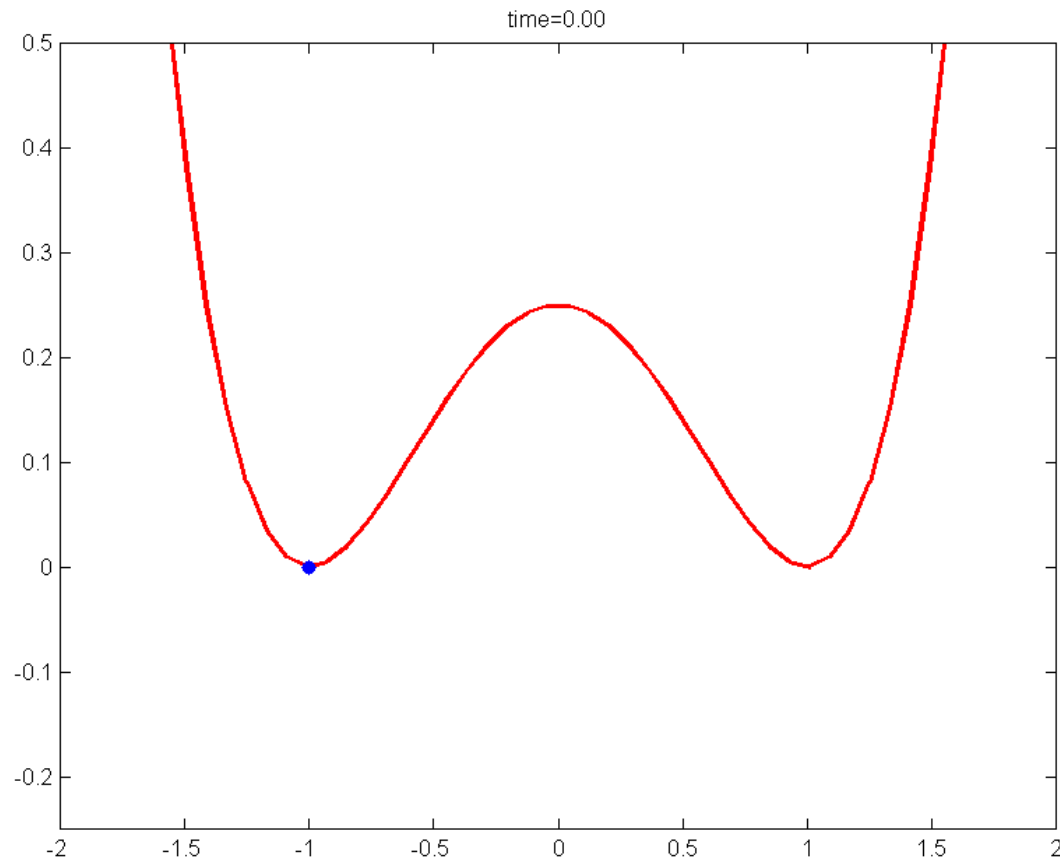


DOE of a  $A_3B$  compound  
with  $M_H / M_L = 50$



DB is localized on a **single light atom** vibrating along **<100> direction** with the frequency of **227 THz**, which is **inside the phonon gap**. Shown is the x-displacement of the light atom as the function of time. DB has very large amplitude of **0.4 angstrom**, which should be compared to the lattice parameter  **$a=1.35$  angstrom**

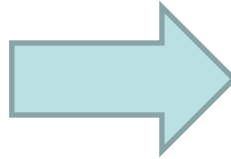
# LAV effect (1): periodic in time modulation of the potential barrier height



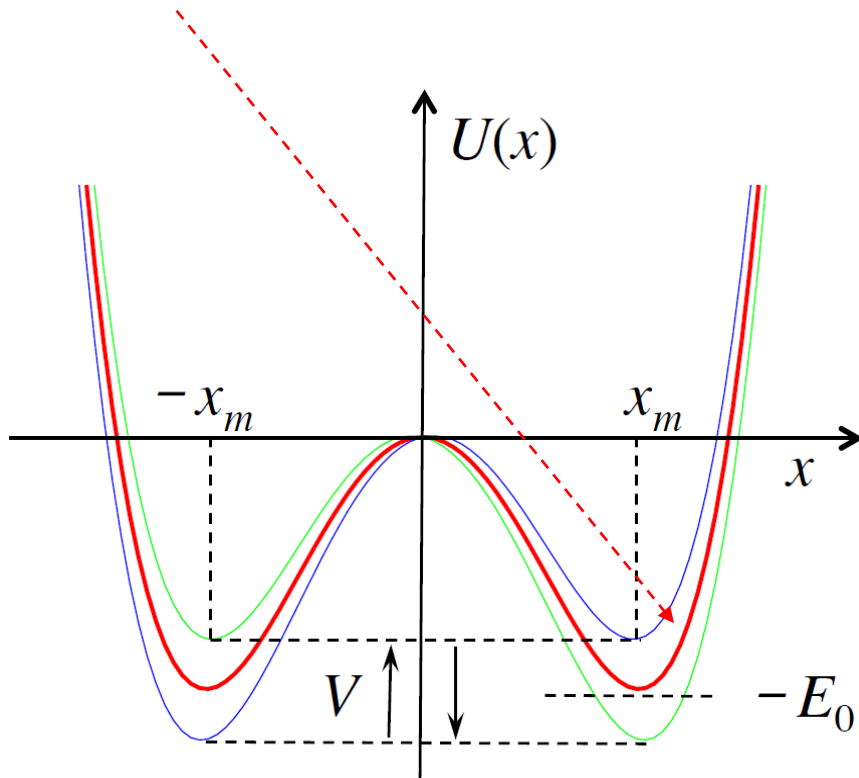
# Reaction-rate theory with account of the crystal anharmonicity

Dubinko, Selyshchev, Archilla, Phys. Rev. E. (2011)

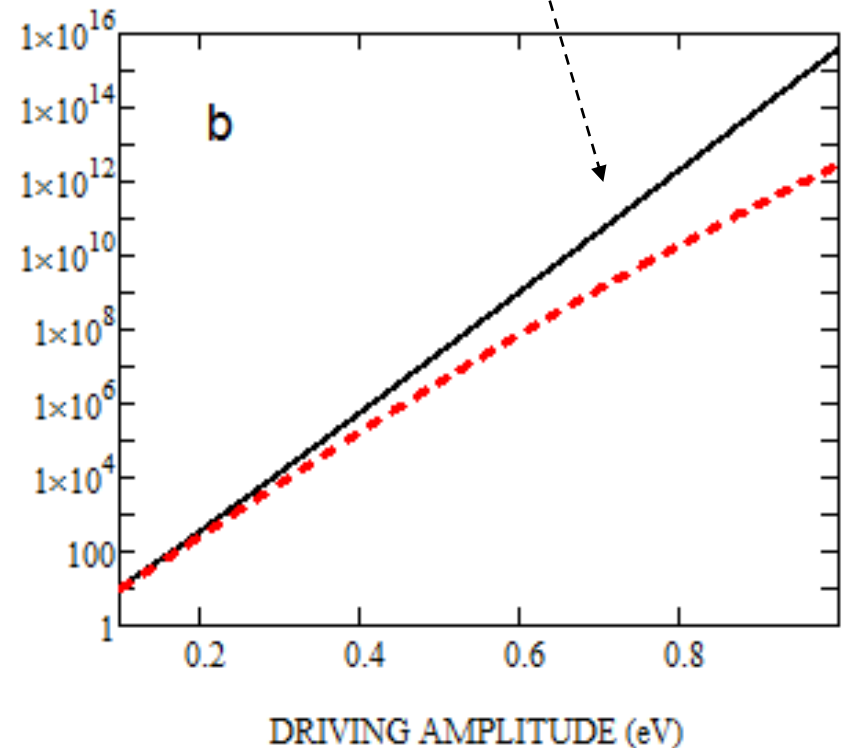
$$U(x,t) = U(x) - (V \cdot x/x_m) \cos(\Omega t)$$



Kramers rate is amplified:  
Bessel function  $I_0(V_m/k_B T)$



AMPLIFICATION FACTOR



**How extend LAV concept  
to include**

**Quantum effects,  
Tunneling**

**?**

# Tunneling as a classical escape rate induced by the vacuum zero-point radiation, [A.J. Faria](#), [H.M. Franca](#), [R.C. Sponchiado](#) Foundations of Physics (2006)

The Kramers theory is extended in order to take into account the action of the thermal and **zero-point oscillation (ZPO)** energy.

$$R_K = \frac{\omega_0}{2\pi} \exp\left[-E_0/D(T)\right]$$

$$D(T) = E_{ZPO} \coth(E_{ZPO}/k_B T) \approx \begin{cases} E_{ZPO}, & T \rightarrow 0 \\ k_B T, & T \gg E_{ZPO}/k_B \end{cases}$$

T – temperature is a measure of *thermal* noise strength

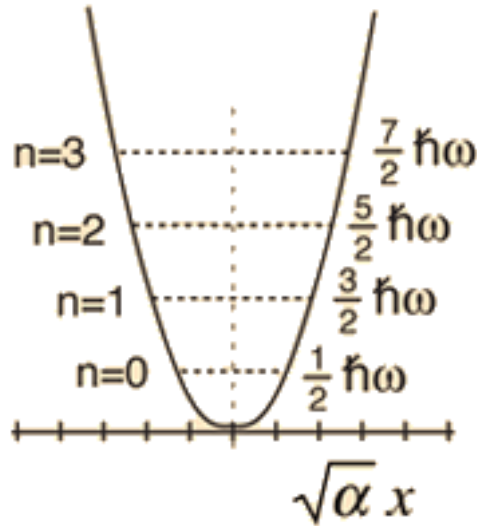
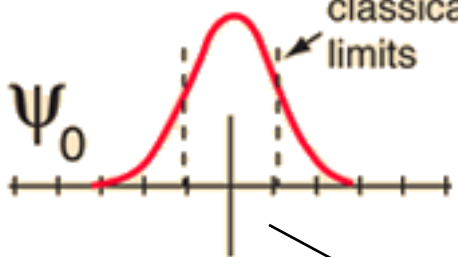
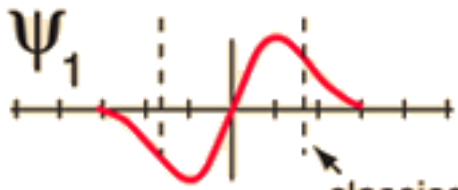
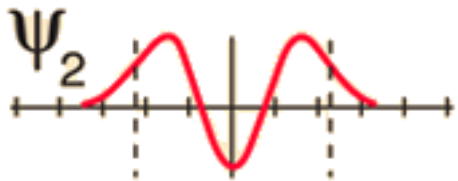
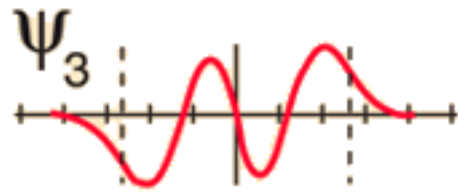
$$E_{ZPO} = \frac{\hbar\omega_0}{2} \quad - \text{ZPO energy is a measure of } \textit{quantum} \text{ noise strength}$$

When we heat the system we increase temperature, i.e. we increase the *thermal* noise strength

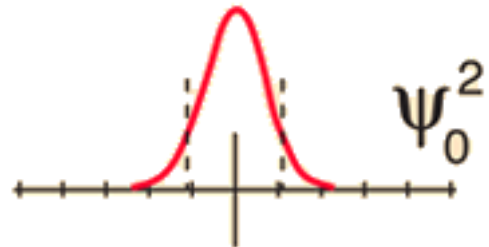
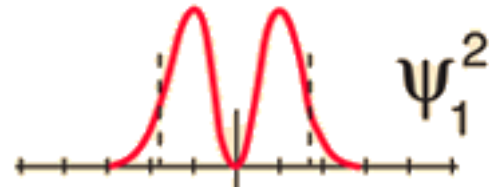
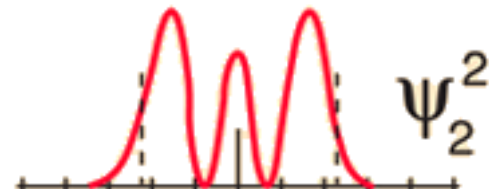
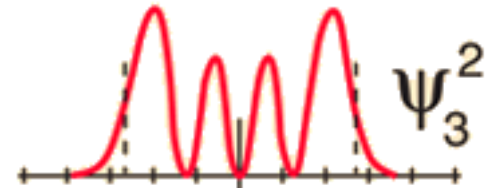
Can we increase the *quantum* noise strength, i.e. ZPO energy?

# Stationary harmonic potential

$$\langle E \rangle_n = \hbar\omega_0 \left( n + \frac{1}{2} \right)$$

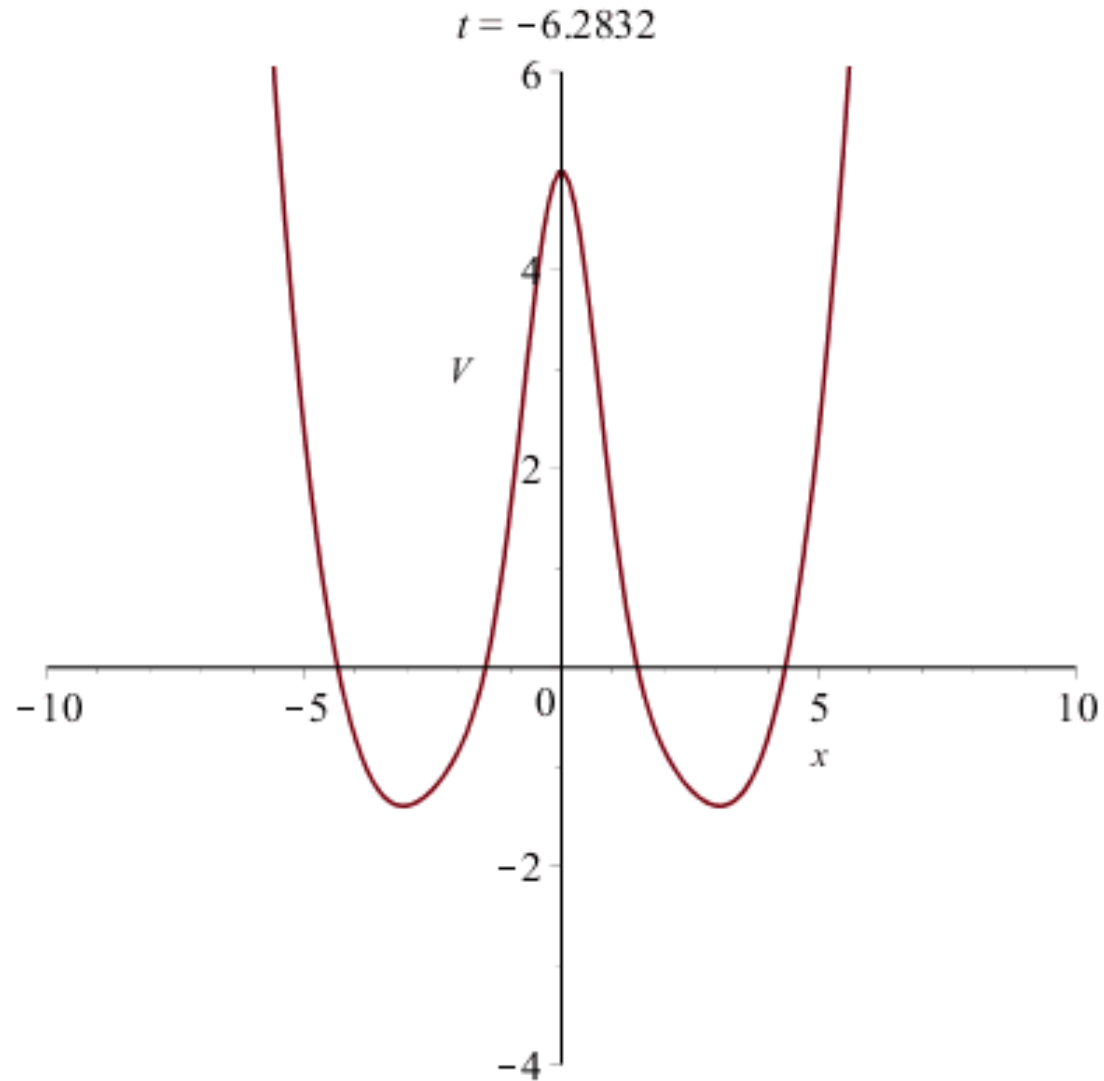


Harmonic oscillator potential and wavefunctions



$$E_{ZPO} = \frac{\hbar\omega_0}{2}$$

Time-periodic modulation of the **double-well** shape changes (i) eigenfrequency and (ii) position of the wells



# Quasi-energy in time-periodic systems

Consider the Hamiltonian which is periodic in time.

$$i\hbar \frac{\partial \psi}{\partial t} = \hat{H} \psi \quad \hat{H}(t+T) = \hat{H}(t)$$

It can be shown that Schrodinger equation has class of solutions in the form:

$$\psi_{\alpha}(t+T) = \exp(-i\alpha) \psi_{\alpha}(t)$$

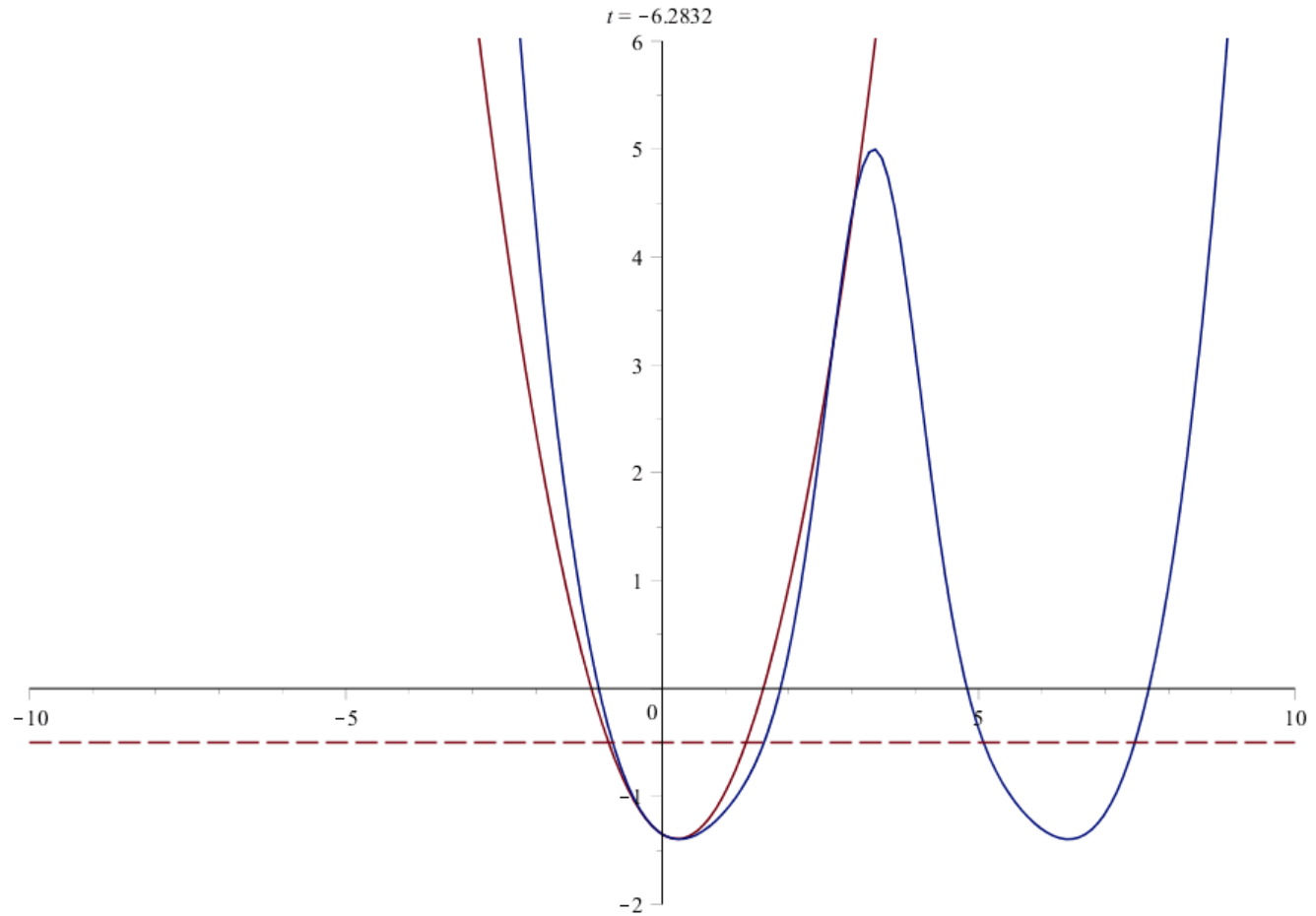
where  $\varepsilon = \frac{\hbar\alpha}{T}$  is the quasi-energy

$$i\hbar \frac{\partial}{\partial t} \psi(x,t) = -\frac{\hbar^2}{2m} \frac{\partial^2}{\partial x^2} \psi(x,t) + \frac{m\omega^2(t)}{2} x^2 \psi(x,t)$$

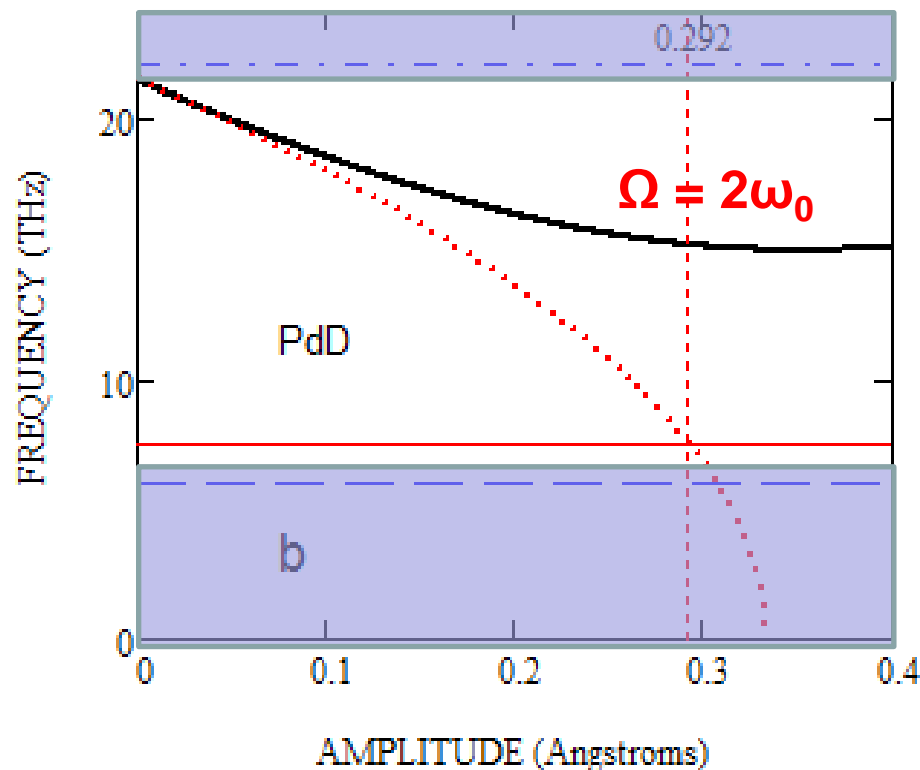
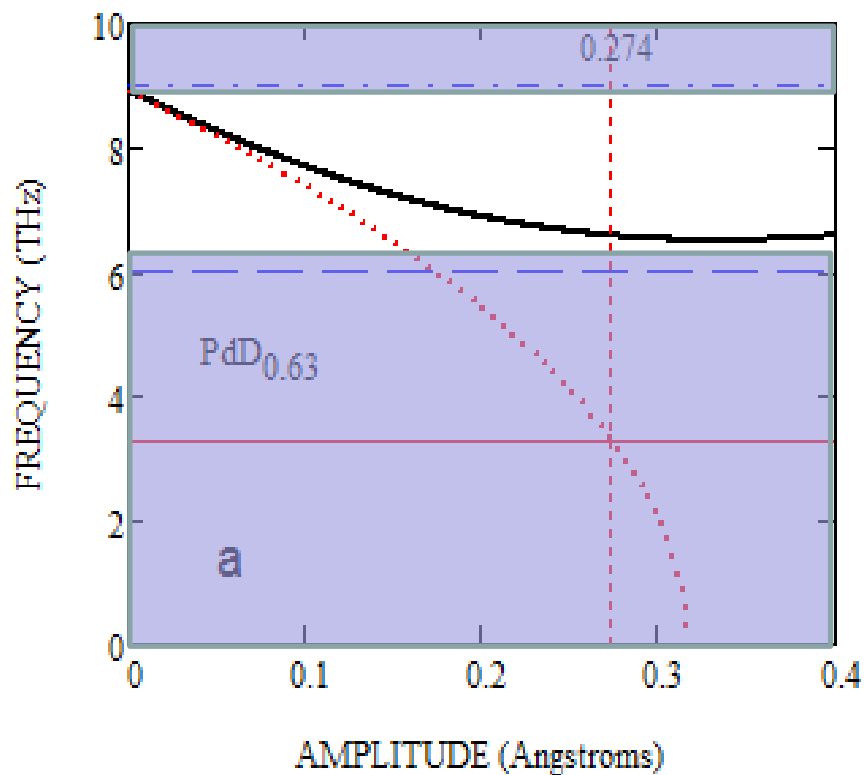
$$\varepsilon_n = \left( n + \frac{1}{2} \right) \lambda(\omega(t))$$

Time-periodic driving of the harmonic oscillator with non resonant frequencies  $\Omega \neq 2\omega_0$  renormalizes its energy spectrum, which remains equidistant, but the quasi-energy quantum  $\lambda(\omega(t))$  becomes a function of the driving frequency

# Time-periodic modulation of the double-well shape changes (i) eigenfrequency and (ii) position of the wells



# DB frequency and eigenfrequency of the potential wells of neighboring D ions in PdD (Dubinko, ICCF 19)



DB polarized along the close-packed D-D direction  $\langle 110 \rangle$

- DB frequency
- ⋯ Eigenfrequency
- Upper acoustic phonon edge
- · Lower optic phonon edge
- Resonance frequency

# Parametric resonance with time-periodic eigenfrequency $\Omega = 2\omega_0$

$$i\hbar \frac{\partial \psi}{\partial t} = -\frac{\hbar^2}{2m} \frac{\partial^2 \psi}{\partial x^2} + \frac{m\omega^2(t)}{2} x^2 \psi$$

**Schrödinger equation**

$$\psi(x_0, t_0 = 0) = \frac{1}{\sqrt[4]{2\pi\sigma_0}} \exp\left(-\frac{x_0^2}{4\sigma_0}\right)$$

Initial Gaussian packet  $\sigma_0 = \frac{\hbar}{2m\omega_0}$

**Parametric regime  $\Omega = 2\omega_0$ :**

$$\ddot{x} + \omega_0^2 [1 - g \cos(2\omega_0 t)] x = 0$$

$g \ll 1$  – modulation amplitude

$$\sigma_x(t) = \sigma_0 \cosh\left(\frac{g\omega_0 t}{2}\right) \left[ 1 + \tanh\left(\frac{g\omega_0 t}{2}\right) \sin(2\omega_0 t) \right] \quad \text{dispersion}$$

**ZPO energy:**

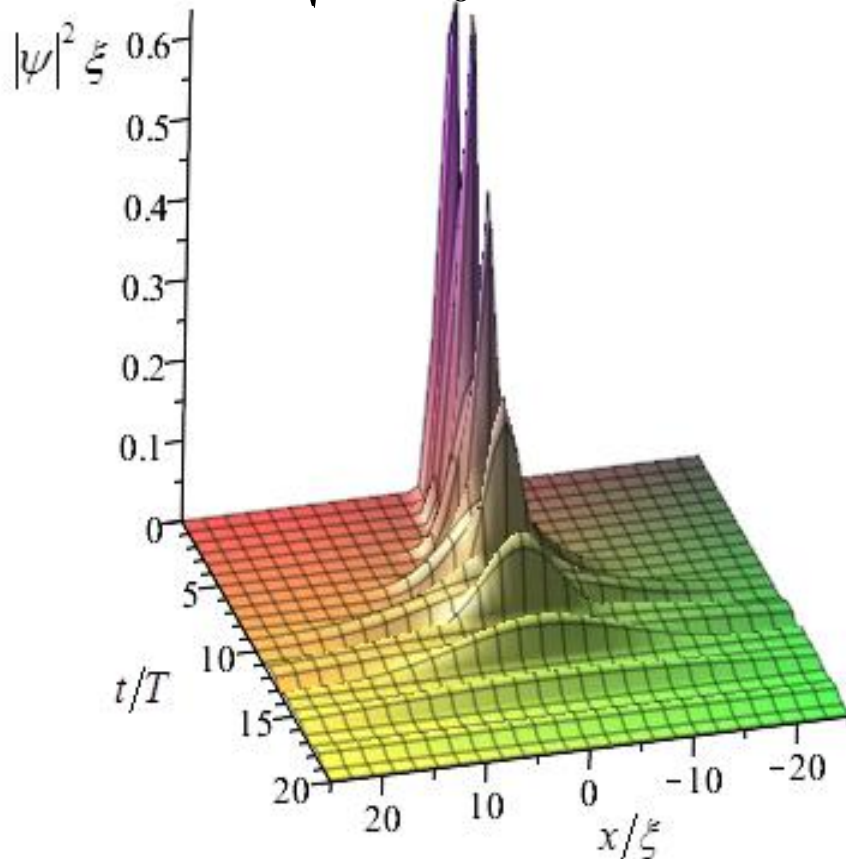
$$E_{ZPO}(t) = \frac{\hbar\omega_0}{2} \cosh\frac{g\omega_0 t}{2}$$

**ZPO amplitude:**

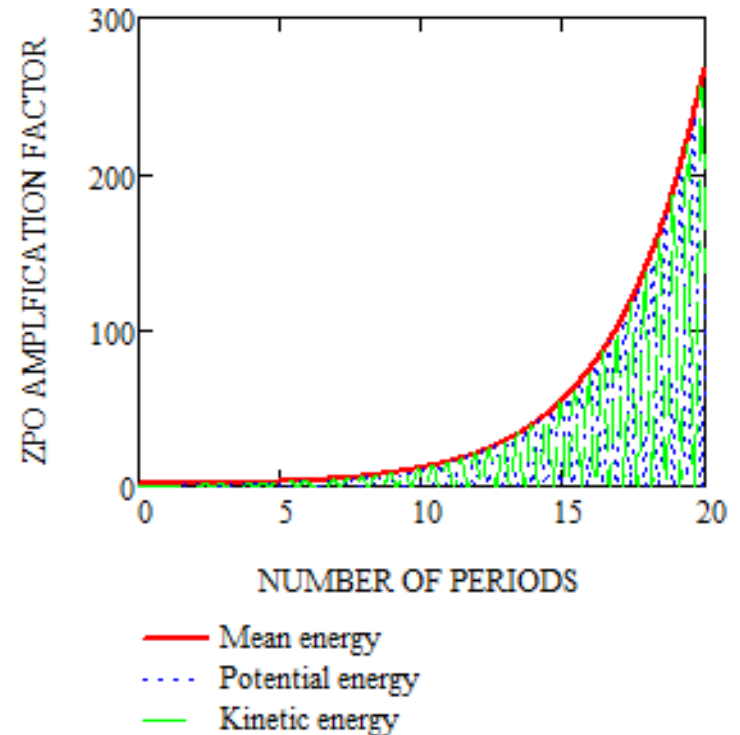
$$\Lambda_{ZPO}(t) = \sqrt{\frac{\hbar}{2m\omega_0} \cosh\frac{g\omega_0 t}{2}}$$

# Non-stationary harmonic potential with time-periodic eigenfrequency $\Omega = 2\omega_0$

$$\Lambda_{ZPO}(t) = \sqrt{\frac{\hbar}{2m\omega_0} \cosh \frac{g\omega_0 t}{2}}$$



$$E_{ZPO}(t) = \frac{\hbar\omega_0}{2} \cosh \frac{g\omega_0 t}{2}$$

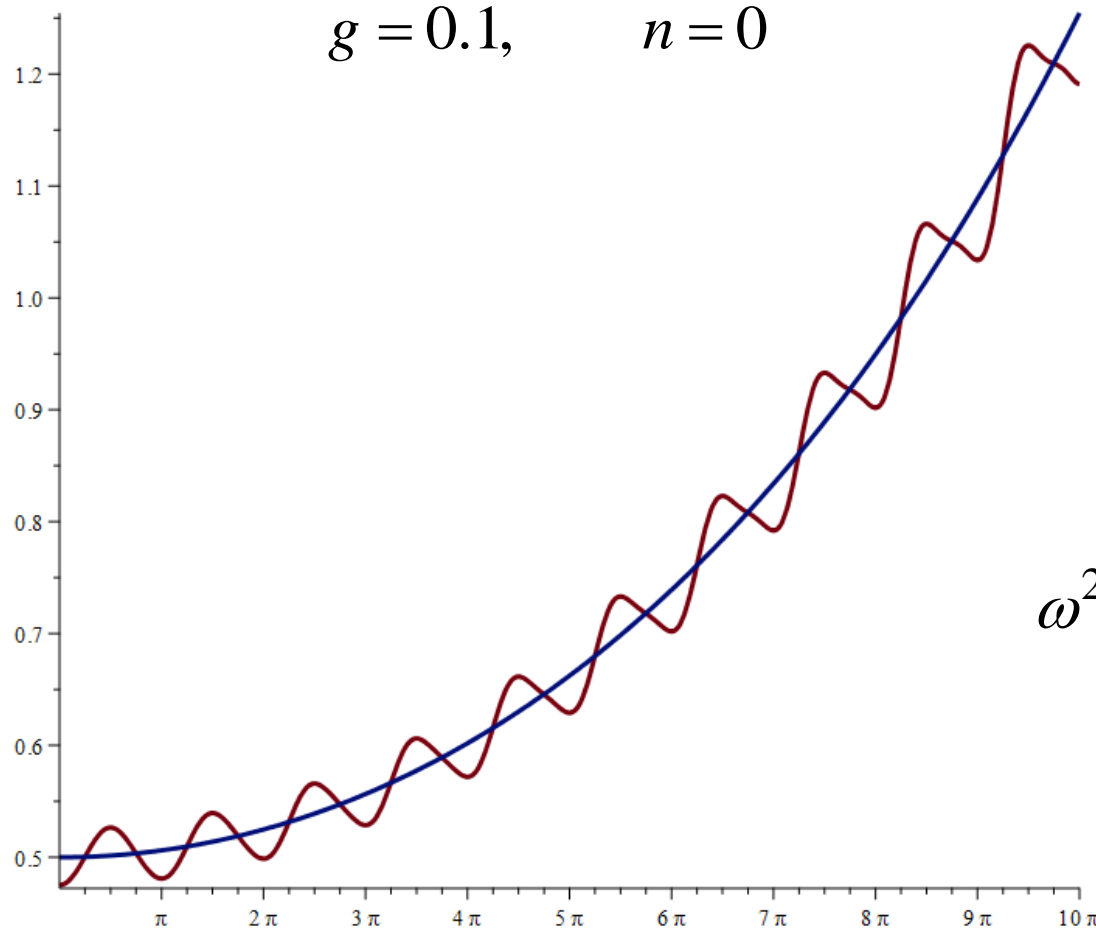


$$\langle E \rangle_{theor}(t) \approx \hbar \omega_0 \left( n + \frac{1}{2} \right) \cosh \frac{g \omega_0 t}{2}$$

$$g \ll 1$$

General case:  $n = 0, 1, 2, \dots$

$$\langle E \rangle_{num}(t) = \frac{\hbar \omega_0}{2} \left( n + \frac{1}{2} \right) \left[ \frac{\dot{Y}^2 + \omega_0^2 \dot{Z}^2}{\omega_0^2} + \frac{\omega^2(t)}{\omega_0^2} (Y^2 + \omega_0^2 Z^2) \right]$$



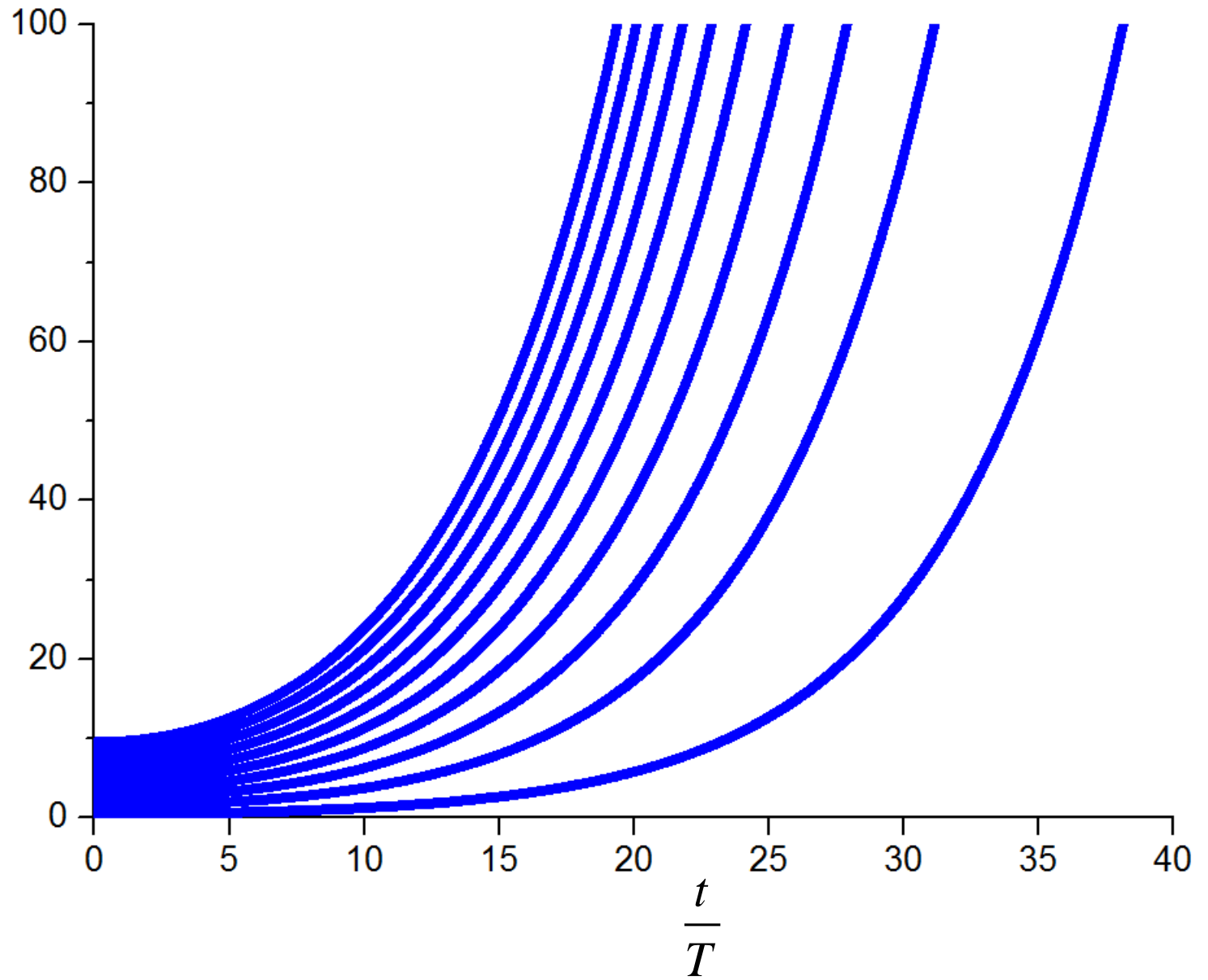
$$\begin{cases} \ddot{Y}(t) + \omega^2(t)Y(t) = 0 \\ \dot{Y}(0) = 0, \quad Y(0) = 1 \end{cases}$$

$$\begin{cases} \ddot{Z}(t) + \omega^2(t)Z(t) = 0 \\ \dot{Z}(0) = 1, \quad Z(0) = 0 \end{cases}$$

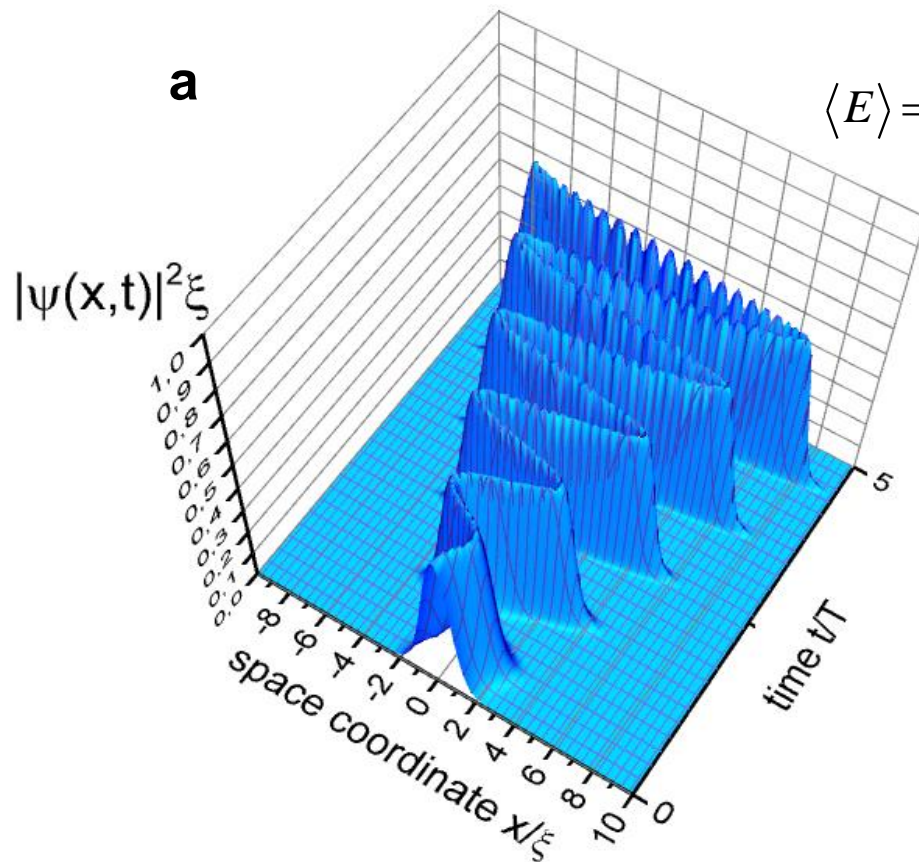
$$\omega^2(t) = \omega_0^2 [1 - g \cos(2\omega_0 t)]$$

$g = 0.1$

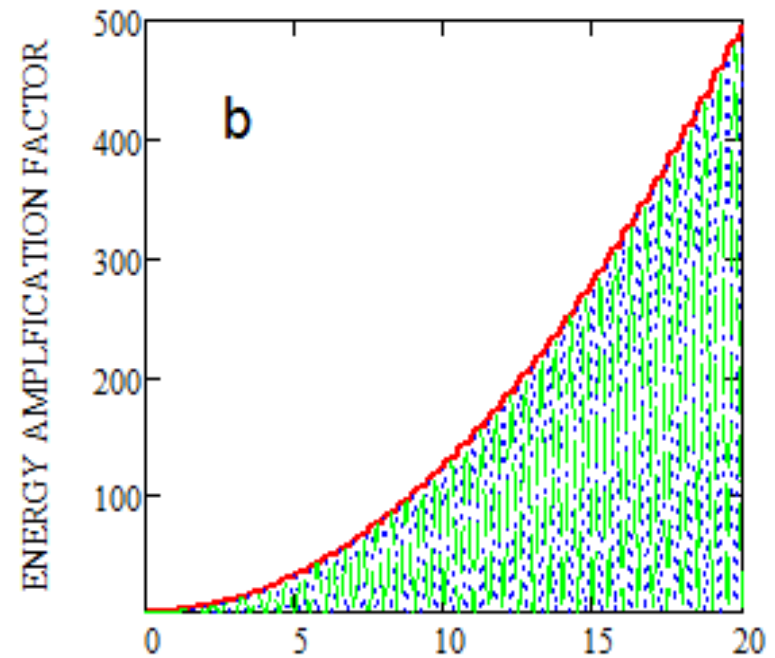
$$\frac{\langle E \rangle_n}{\hbar \omega_0}$$



# Non-stationary harmonic potential with time-periodic shifting of the well position at $\Omega = \omega_0$



$$\langle E \rangle = \frac{\hbar\omega_0}{2} + \frac{(g_A A_{ZPO})^2 m\omega_0^2}{8} \left[ \omega_0^2 t^2 + \omega_0 t \sin 2\omega_0 t + \sin^2 \omega_0 t \right]$$



$$\lambda(t) = \frac{g_A A_{ZPO}}{2} \omega_0 t \left( \cos \omega_0 t - \frac{\sin \omega_0 t}{\omega_0 t} \right)$$

- Mean energy
- · · Potential energy
- · · Kinetic energy

# Well-known and well-forgotten quantum mechanics

W. Heisenberg, “Über den anschaulichen Inhalt der quantentheoretischen Kinematik und Mechanik”, *Z. Phys.*, **43**, 172–198 (1927).

$$\Delta x \Delta p \geq \hbar/2$$

**Uncertainty Relations (UR)**  
Heisenberg (1927)

E. Schrödinger, “Zum Heisenbergschen Unschärfeprinzip”, *Ber. Kgl. Akad. Wiss. Berlin*, **24**, 296–303 (1930).

H. P. Robertson, “A general formulation of the uncertainty principle and its classical interpretation”, *Phys. Rev.*, **35**, 667 (1930).

$$\sigma_x \sigma_p - \sigma_{xp}^2 \geq \hbar^2/4,$$

**Generalization of the UR**  
Schrödinger (1930); Robertson (1930)

$$\sigma_x = \langle (x - \langle x \rangle)^2 \rangle$$

$$\sigma_p = \langle (p - \langle p \rangle)^2 \rangle$$

$$\sigma_{xp} = \langle \hat{x}\hat{p} + \hat{p}\hat{x} \rangle / 2 - \langle x \rangle \langle p \rangle.$$

**Correlator**

# GENERALIZED UNCERTAINTY RELATION AND CORRELATED COHERENT STATES

V.V. DODONOV, E.V. KURMYSHEV and V.I. MAN'KO **Phys. Letters (1980)**

$$\sigma_x \sigma_p \geq \frac{\hbar^2}{4(1-r^2)}, \quad \text{Correlation coefficient} \quad r = \frac{\sigma_{xp}}{\sqrt{\sigma_x \sigma_p}}$$

$$\hbar_{ef} = \frac{\hbar}{\sqrt{1-r^2}}, \quad \text{Effective Plank constant} \quad \hbar_{ef} \xrightarrow{r \rightarrow 1} \infty$$

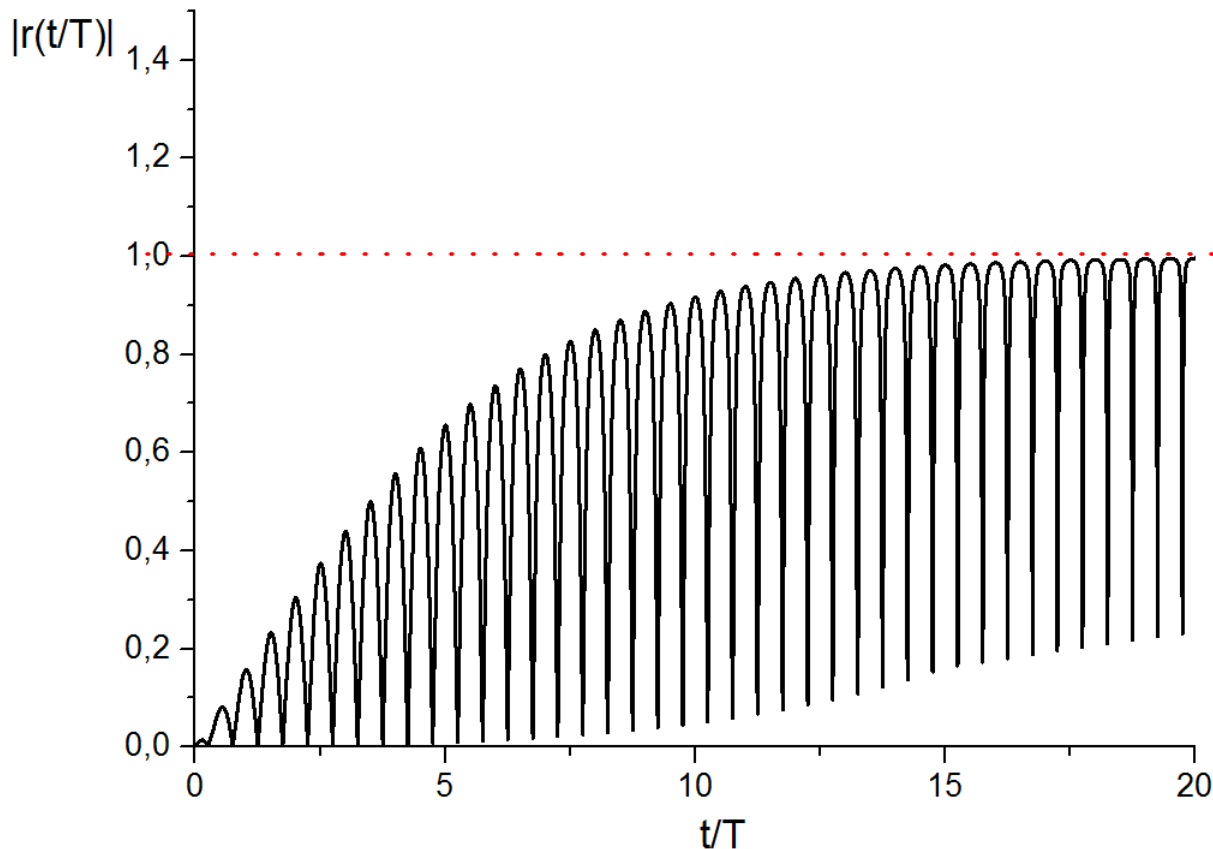
**Can CORRELATIONS make the barrier transparent ?!**

Vysotskii et al, Eur. Phys. J. A (2013):

$$G_{ef} \approx \exp \left\{ -\frac{2}{\hbar_{ef}} \int_{R_0}^{R_c} dr \sqrt{2\mu(V(r) - E)} \right\} \xrightarrow{r \rightarrow 1, \hbar_{ef} \rightarrow \infty} 1$$

# Correlations Coefficient for the parametric resonance $\Omega = 2\omega_0$

$$r_{xp} = r_{xp}(t) = \frac{\sinh\left(\frac{g\omega_0 t}{2}\right) \cos(2\omega_0 t)}{\sqrt{1 + \left[\sinh\left(\frac{g\omega_0 t}{2}\right) \cos(2\omega_0 t)\right]^2}} + O(g)$$

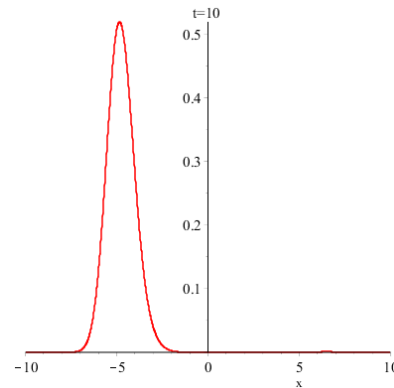
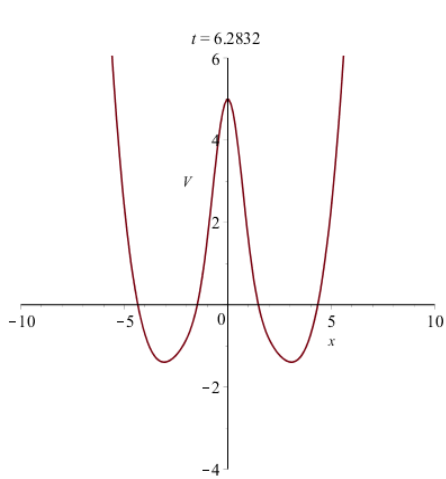


$$g = 0.1$$

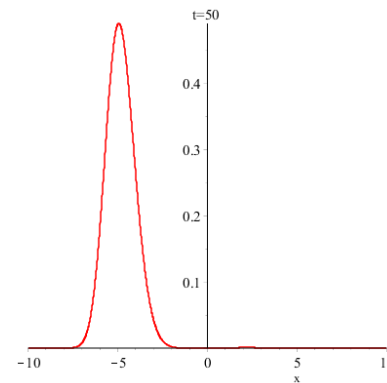
$$T = \frac{2\pi}{2\omega_0}$$

# Tunneling: Numerical solution of Schrödinger equation

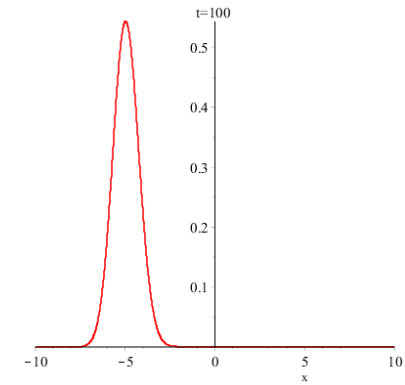
Stationary:  $t_{\text{Kramers}} \sim 10^5$  cycles at  $V_{\text{barrier}} = 12E_0$



10 cycles

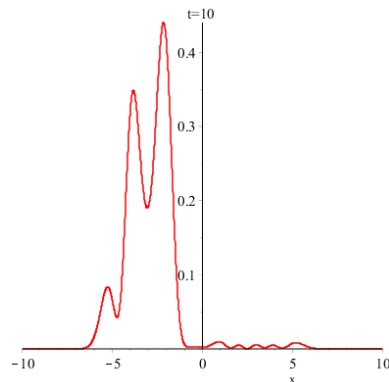
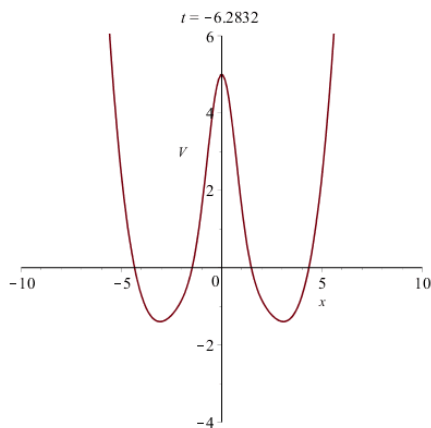


50 cycles

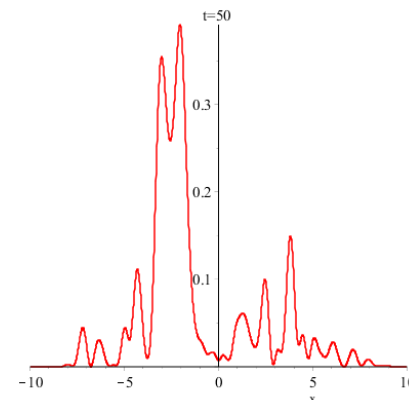


100 cycles

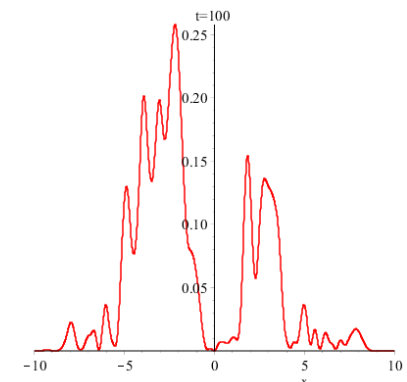
Time-periodically driven:  $\Omega = 1.5 \omega_0$ ,  $g = 0.2$



10 cycles



50 cycles



100 cycles

# Extreme example – Low Energy Nuclear Reactions (**LENR**)

# Why LENR is unbelievable?

G. Gamow, "Zur Quantentheorie des Atomkernes", *Z. Phys.*, 51, 204–212 (1928).

$$G \approx \exp \left\{ -\frac{2}{\hbar} \int_{r_0}^{R_c} dr \sqrt{2\mu(V(r) - E)} \right\} \quad \text{Gamow factor}$$

$r_0 \sim 3 \text{ fm}$  Nuclear radius deduced from scattering experiments

$$V(R_0) = \frac{e^2}{r_0} \approx 450 \text{ keV} \quad \Rightarrow \quad \text{Coulomb barrier}$$

At any crystal  
Temperature:

$$E \ll V(r_0) \Rightarrow G \approx 10^{-2760}$$

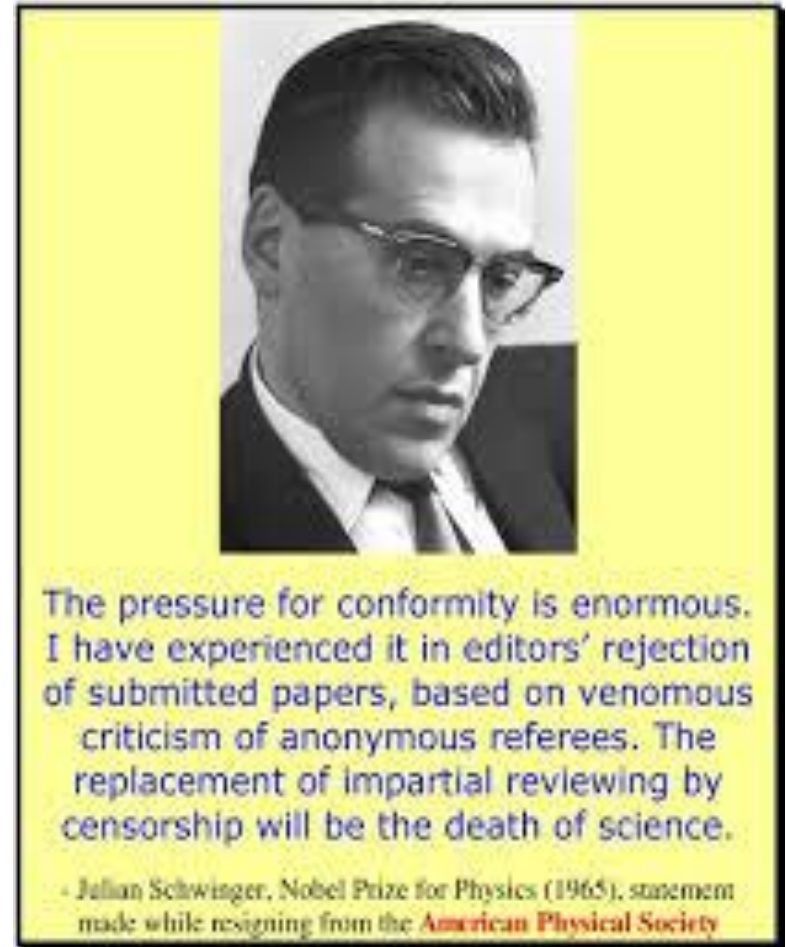
**HOWEVER, is** the Coulomb barrier that huge in the lattice ?

Willis Eugene *Lamb*  
Nobel Prize 1955



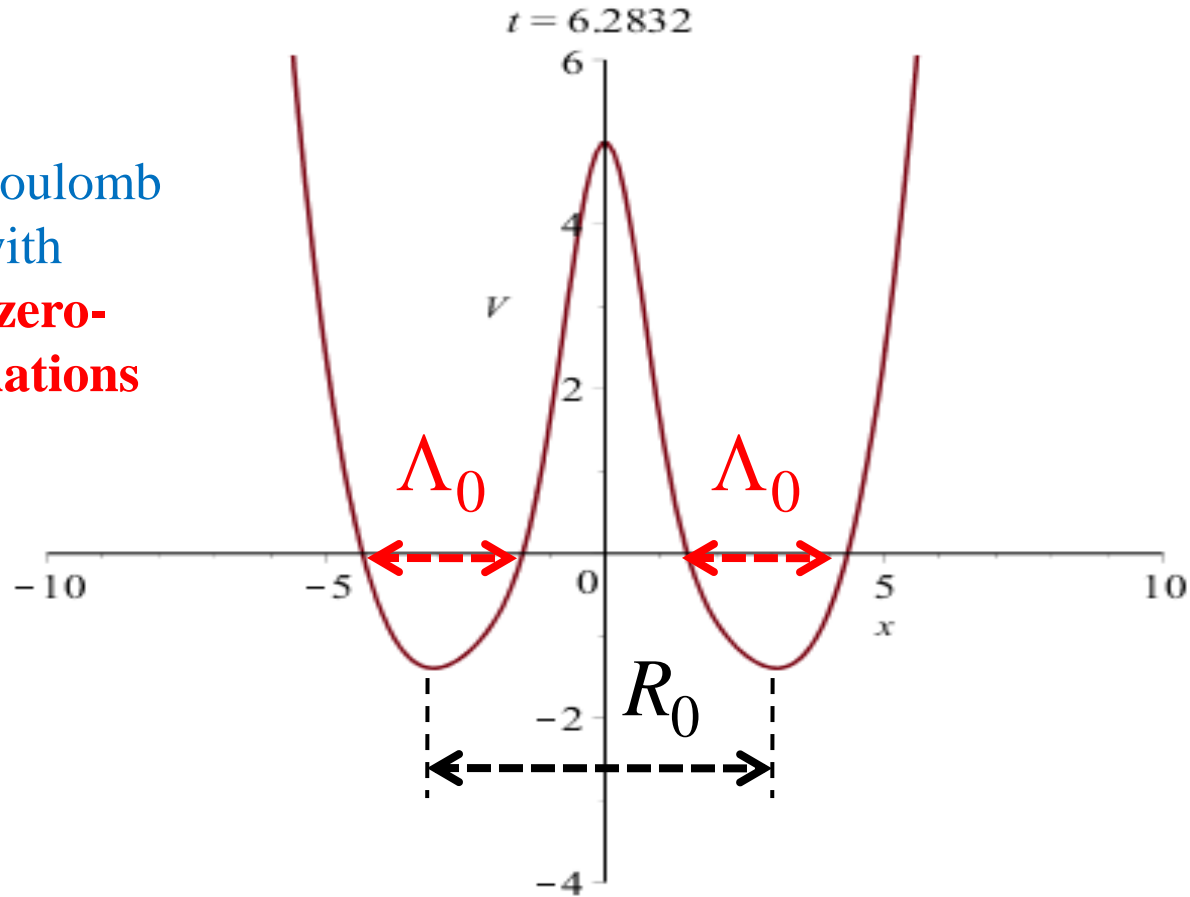
R.H. Parmenter, **W.E. Lamb**,  
**Cold fusion in Metals (1989)**  
*Electron screening*

Julian Schwinger  
Nobel Prize 1965



**J. Schwinger**, **Nuclear Energy in an Atomic Lattice (1990)**  
*Lattice screening*

Effective Coulomb repulsion with account of **zero-point oscillations**



$${}_0\langle V_c(r) \rangle_0 = \frac{e^2}{r} \sqrt{\frac{2}{\pi}} \int_0^{r/\Lambda_0} dx \exp\left(-\frac{1}{2}x^2\right) \approx \begin{cases} r \gg \Lambda_0 : \frac{e^2}{r} \\ r \ll \Lambda_0 : \left(\frac{2}{\pi}\right)^{1/2} \frac{e^2}{\Lambda_0} \sim \mathbf{100 \text{ eV} (!!!)} \end{cases}$$

**J. Schwinger**, *Nuclear Energy in an Atomic Lattice* The First Annual Conference on Cold Fusion. University of Utah Research Park, Salt Lake City (**1990**)

**D-D fusion rate in Pd-D lattice:**  $\nu_{D-D} = \frac{1}{T_0} = (2\pi/\hbar)_0 \langle V \delta(H - E) V \rangle_0$

$T_0$  is the mean lifetime of the *phonon vacuum* state before releasing the nuclear energy **directly** to the lattice (**no radiation!**):

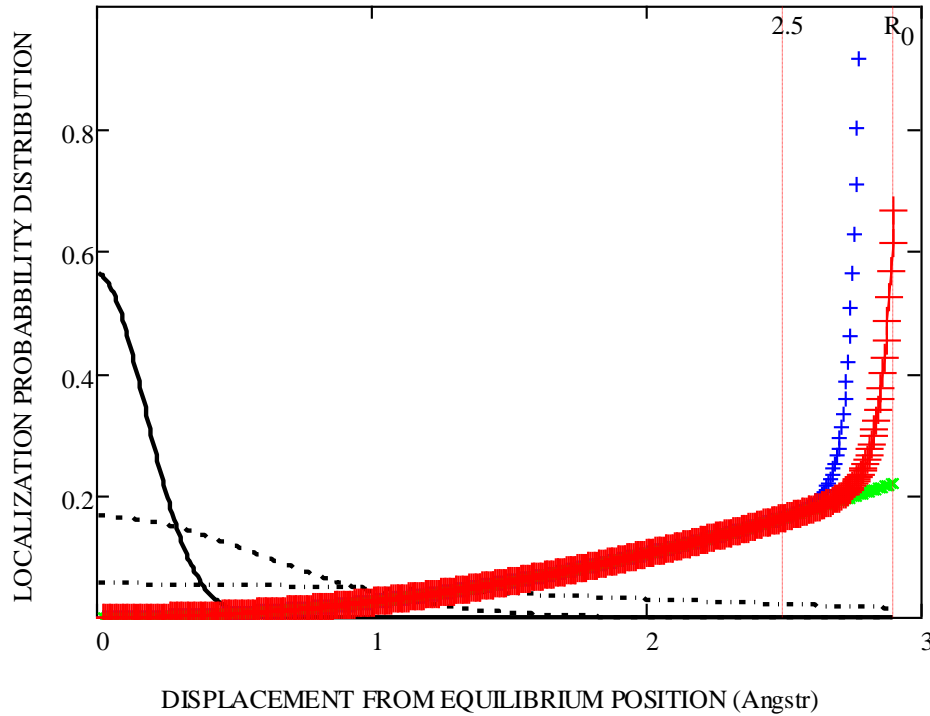
$$\frac{1}{T_0} \approx 2\pi\omega_0 \left( \frac{2\pi\hbar\omega_0}{E_{nucl}} \right)^{\frac{1}{2}} \left( \frac{r_{nucl}}{\Lambda_0} \right)^3 \exp \left[ -\frac{1}{2} \left( \frac{R_0}{\Lambda_0} \right)^2 \right] \sim 10^{-19} s^{-1} \div 10^{-30} s^{-1}$$

$\Lambda_0 = 0.1\text{\AA}$ 
 $R_0 = 0.94\text{\AA} \div 2.9\text{\AA}$

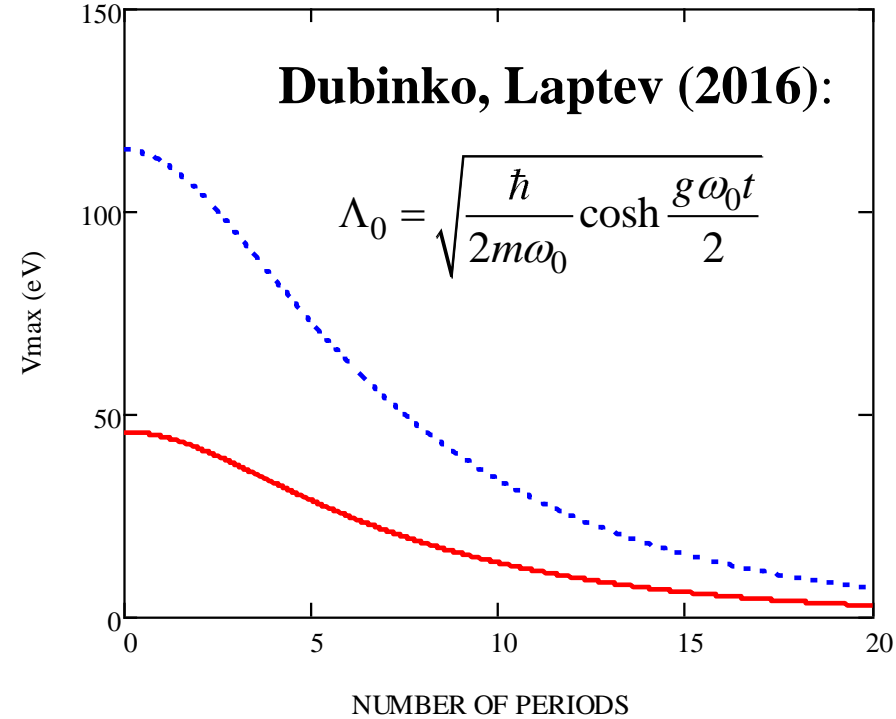
Schwinger, **Nuclear Energy in an Atomic Lattice** I, Z. Phys. D 15, 221 (1990).

Parmenter, Lamb, **Cold fusion in Metals**, Proc. Natl. Acad. Sci. USA, v. 86, 8614-8617 (1989).

$$V_{eff}(r) \approx \frac{m\omega_0^2}{2} r^2 + \frac{e^2}{R_0 - r} \exp\left(-\frac{R_0 - r}{\lambda_D}\right) \sqrt{\frac{2}{\pi}} \int_0^{(R_0 - r)/\Lambda_0} dx \exp\left(-\frac{1}{2} x^2\right)$$



- N=0
- - - N=10
- · · N=17
- +++ Effective potential (x10 eV) by eq. (44) [P&L]
- x x x Harmonic potential (x10 eV)
- + + + Effective potential (x10 eV) at N=17 by eq. (45) [Schwinger]



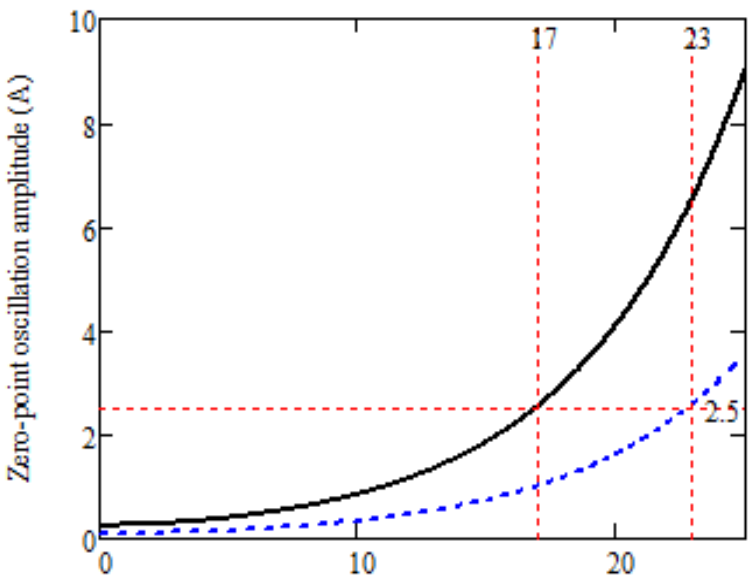
- \$w\_0=50\$ THz (Rowe et al [19])
- · · \$w\_0=320\$ THz (Schwinger [21])

**Schwinger**, *Nuclear energy in an atomic lattice*. Proc. Cold Fusion Conf. (1990)

**Dubinko, Laptev**, *Chemical and nuclear catalysis driven by LAVs*, LetMat (2016)

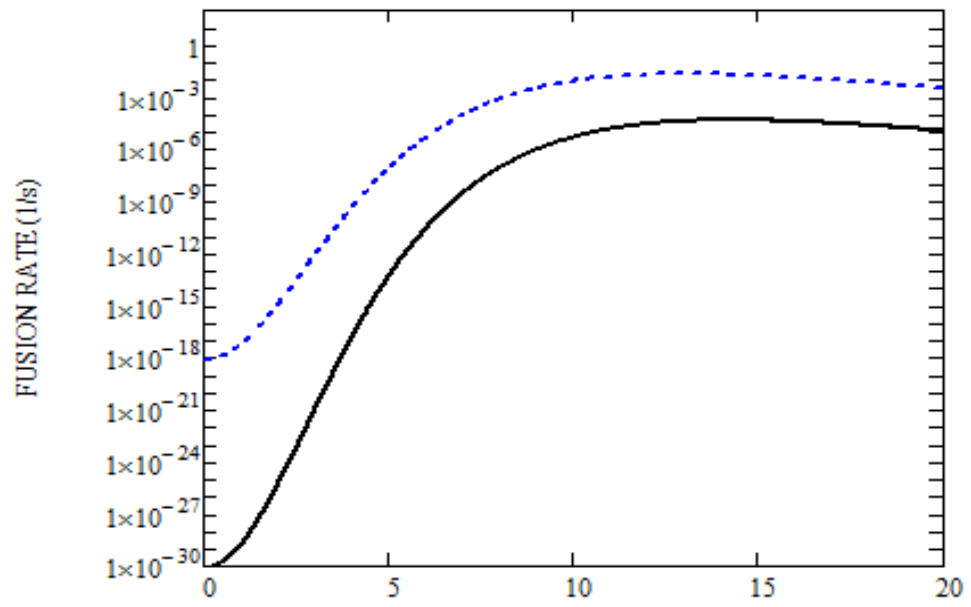
$$\frac{1}{T} \approx 2\pi\omega_0 \left( \frac{2\pi\hbar\omega_0}{E_{nucl}} \right)^{\frac{1}{2}} \left( \frac{r_{nucl}}{\Lambda} \right)^3 \exp \left[ -\frac{1}{2} \left( \frac{R_0}{\Lambda_0} \right)^2 \right]$$

$$\Lambda_0 = \left\{ \begin{array}{l} \sqrt{\frac{\hbar}{2m\omega_0}} = const \\ \sqrt{\frac{\hbar}{2m\omega_0} \cosh \frac{g\omega_0 t}{2}} \end{array} \right\}$$



NUMBER OF PERIODS

— w0= 50 THz (Rowe et al [19])  
 - - - w0=320THz (Schwinger [21])

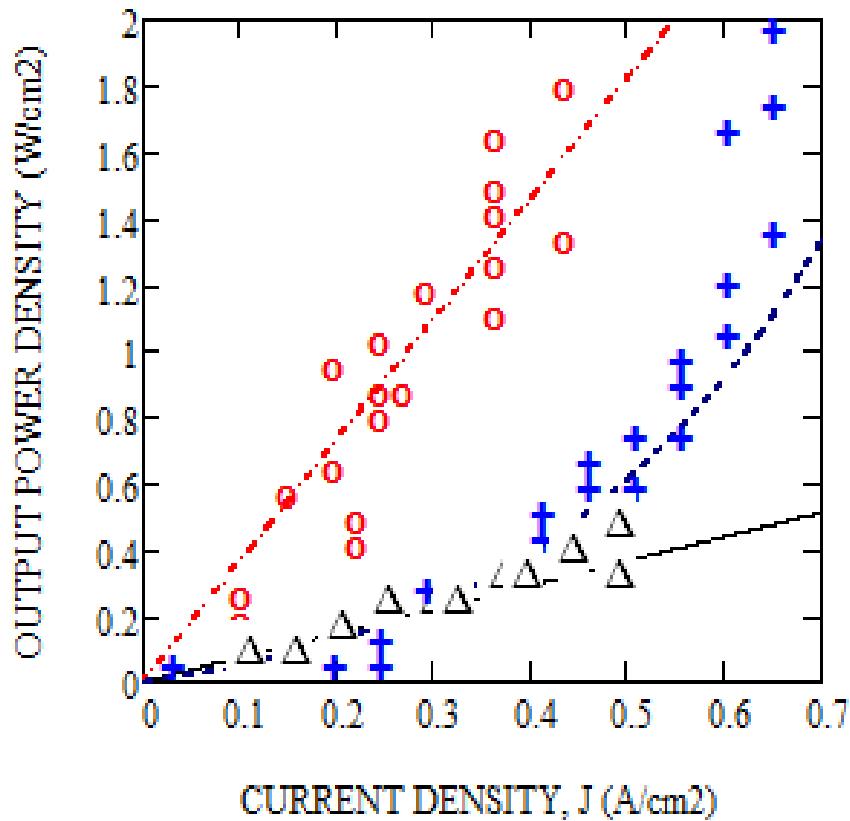


NUMBER OF PERIODS

— w0=50 THz; PdD: R0=2.9A  
 - - - w0=320 THz; PdD2: R0=0.94A (Schwinger)

# LENR power density under D<sub>2</sub>O electrolysis

$$P_{D-D}(T, J) = K_{DB}^J(E_{DB}^*, T, J) E_{D-D}$$



Parameter	Table 1	Value
D-D equilibrium spacing in PdD, b (Å)		2.9
DB excitation efficiency, $k_{eff}$		$10^{-10}$
Fusion energy, (MeV)		23.8
Mean DB energy, (eV)		1
DB oscillation frequency, $\omega_{DB}$ (THz)		20
<b>Critical DB lifetime, <math>\tau_{DB}</math> (ps/cycles)</b>		<b>10/100</b>
Quodon excitation energy (eV)		0.8
Quodon excitation time, $\tau_{ex}$ (ps/cycles)		1/10
Quodon propagation range, $l_q$ (nm)		2.9
Cathod size/thickness (mm)		5

**BNC** can provide up to  $10^{14}$  “collisions” per cm<sup>3</sup> per second

Where to look for  
Nuclear Active Environment?

Small Energy Gap  
is required for

LAV formation

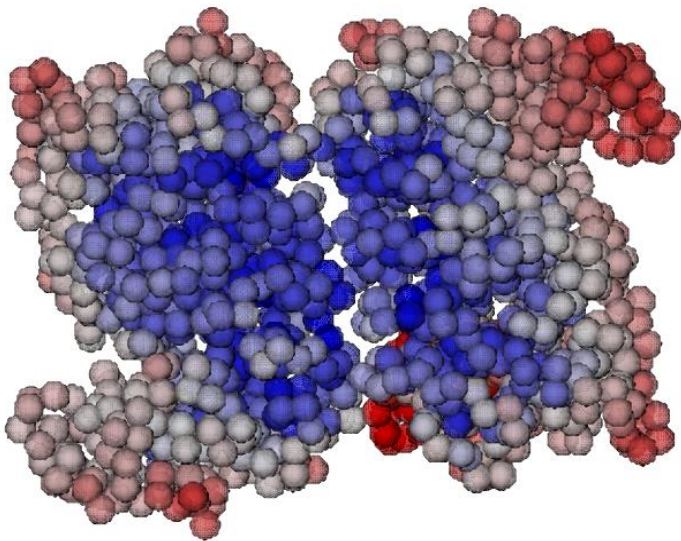


Nuclear Active Environment

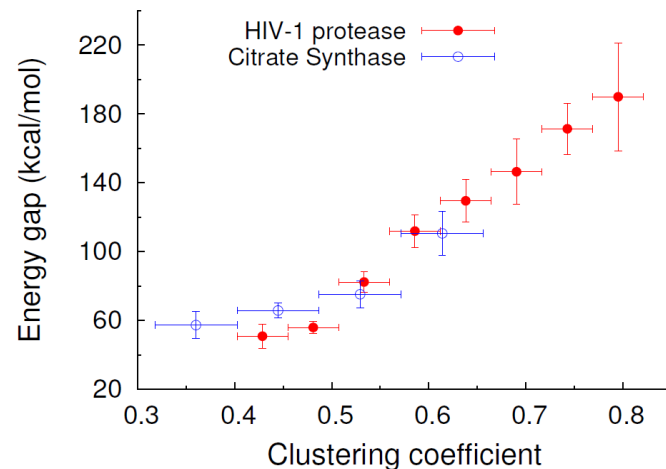
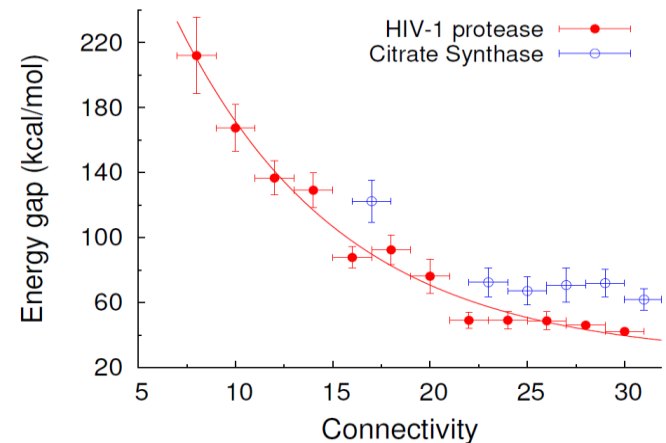
# Chemical and Nuclear catalysis

## the role of disorder

“Cracks and small particles are the Yin and Yang of the cold fusion environment” E. Storms

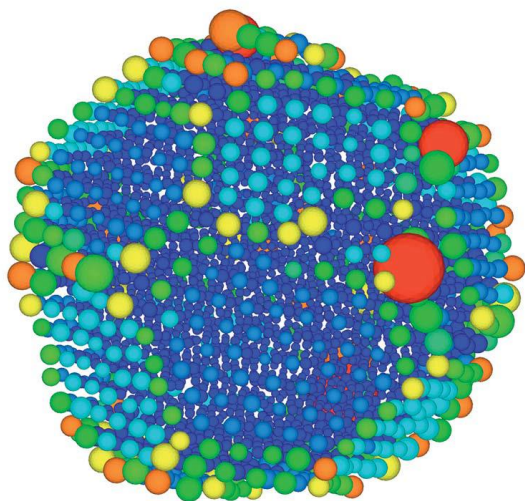
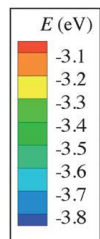


Structure of dimeric citrate synthase (PDB code 1IXE). Only  $\alpha$ -carbons are shown, as spheres in a color scale corresponding to the crystallographic B-factors, from smaller (blue) to larger (red) fluctuations [Dubinko, Piazza, 2014]

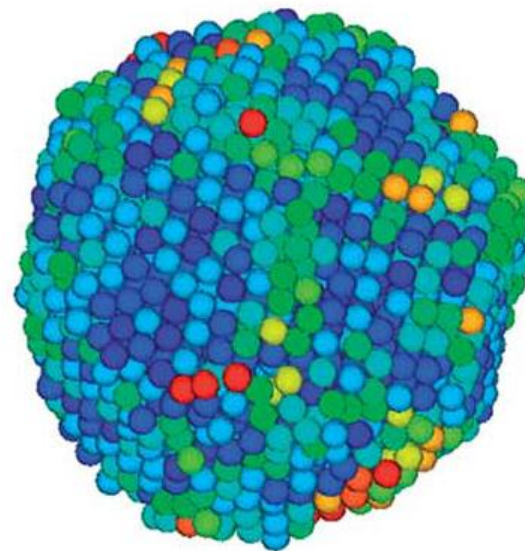


# Chemical and Nuclear catalysis

*Nickel nanoparticles*, Zhang and Douglas (2013)

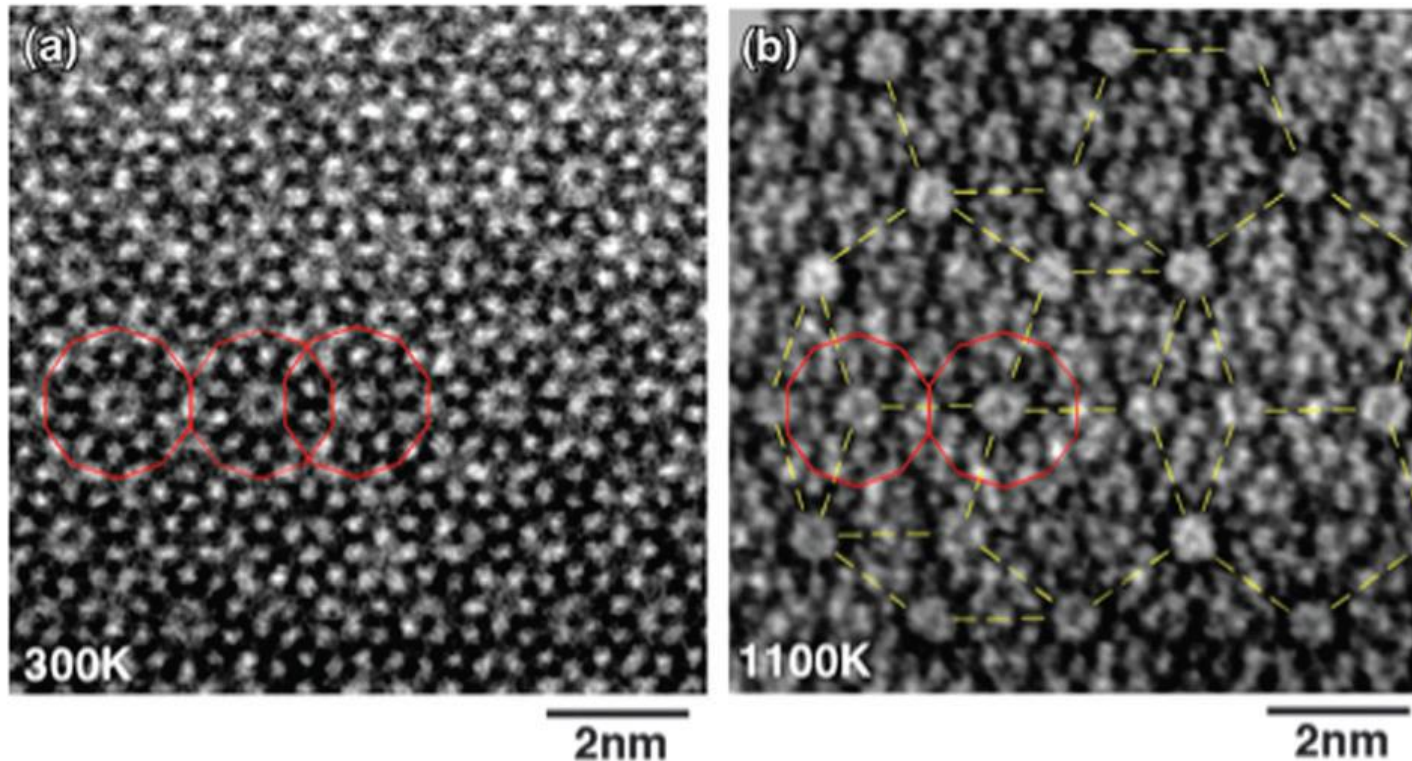


Atomic configuration of a Ni nanoparticle of 2899 atoms at  $T = 1000$  K. The atoms are colored based on the potential energy and their size is proportional to Debye–Waller factor. Potential energy and DWF are time averaged over a 130 ps time window, corresponding to the time interval during which the strings show maximum length.

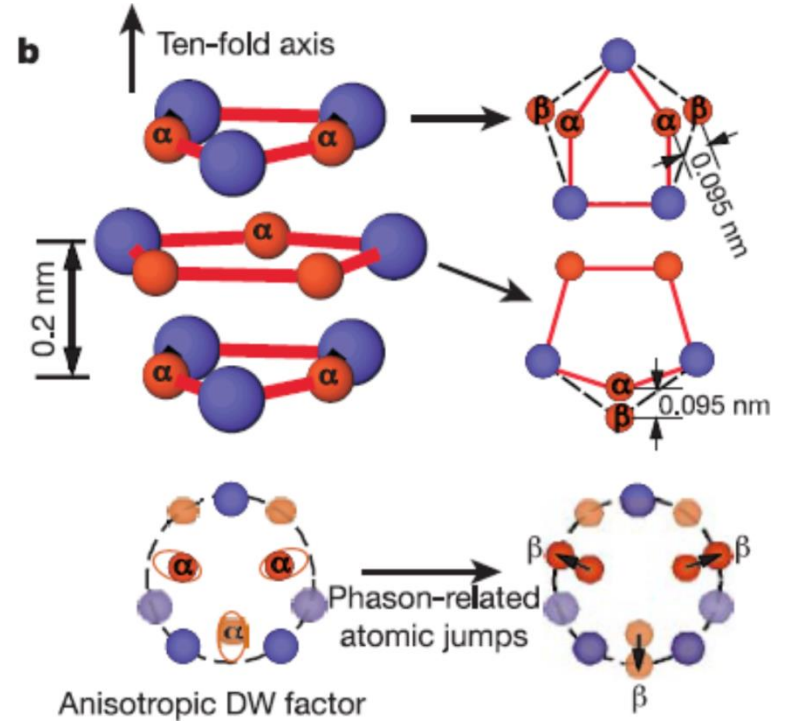
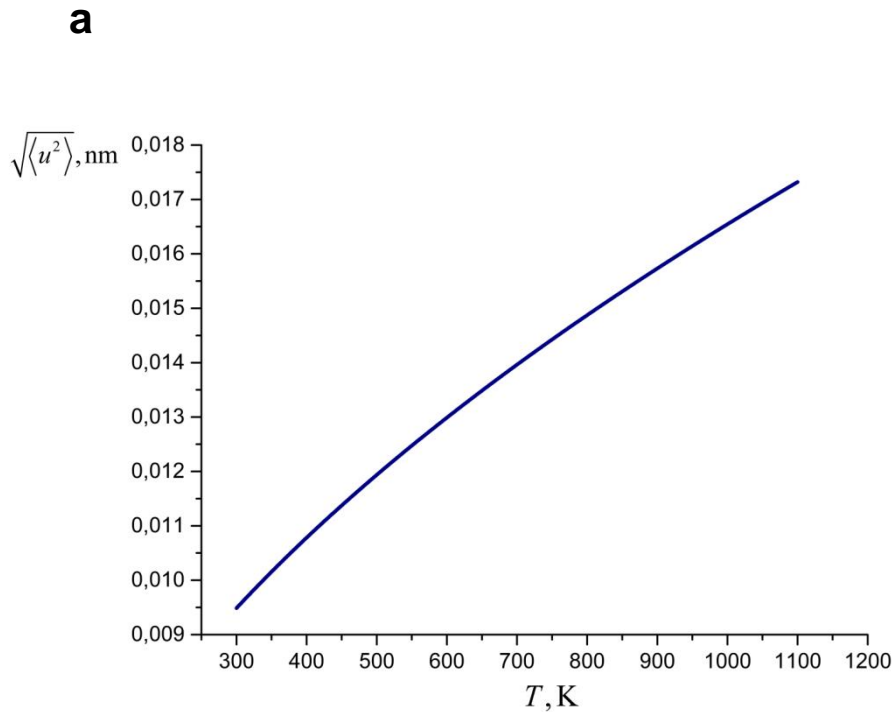


Map of the local Debye–Waller factor showing the heterogeneity of the atomic mobility at a temperature of 1450 K. Regions of high mobility string-like motion are concentrated in filamentary grain boundary like domains that separate regions having relatively strong short-range order.

E. Abe, S.J. Pennycook, A.P. Tsai, *Direct observation of a local thermal vibration anomaly in a quasicrystal*, Nature (London) 421 (2003) 347-350



STEM images of LAVs of the decagonal  $\text{Al}_{72}\text{Ni}_{20}\text{Co}_8$  at (a) 300 K and (b) 1100 K, according to Abe et al. Connecting the center of the 2 nm decagonal clusters (red) reveals significant temperature-dependent contrast changes, a pentagonal quasiperiodic lattice (yellow) with an edge length of 2 nm can be seen in (b).



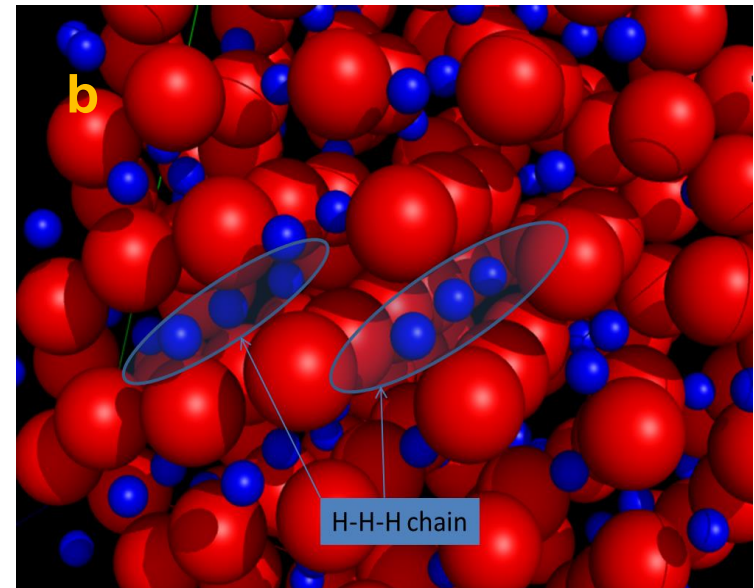
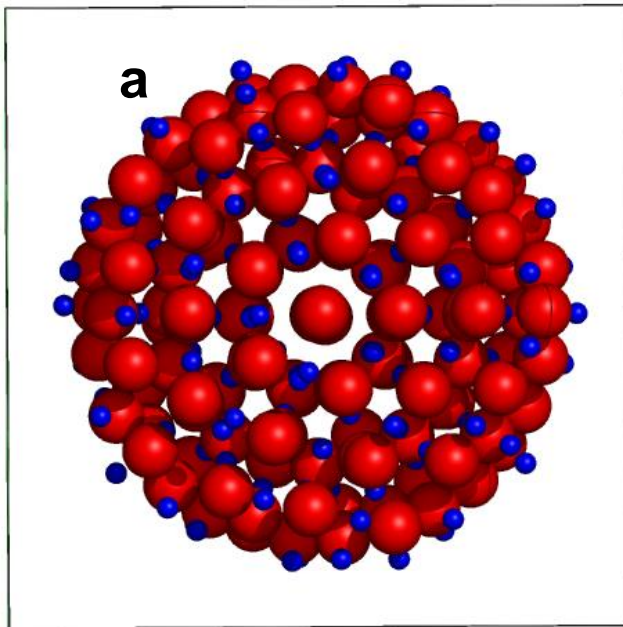
(a) **LAV amplitude** dependence on temperature in  $\text{Al}_{72}\text{Ni}_{20}\text{Co}_8$ , fitted by two points at 300 K and 1100 K, according to Abe et al. The maximum LAV amplitude at 1100K = 0.018 nm.

(b) **LAVs give rise to phasons** at  $T > 990$  K, where a phase transition occurs, and additional quasi-stable sites  $\beta$  arise near the sites  $\alpha$ . The phason amplitude of 0.095 nm is an order of magnitude larger than that of LAVs.

# Chemical and Nuclear catalysis

## DFT modeling of nanoclusters of Pd-H(D)

Terentyev, Dubinko (2015)



**(a)** Structure of Pd-H cluster containing 147 Pd and 138 H atoms having minimum free energy configuration, replicated using the method and parameters by Calvo et al; **(b)** H-H-H chains in the nanocluster, which are viable sites for LAV excitation

**Magic clusters** are clusters of certain ("magic") sizes, which, due to their specific structure, have increased stability compared to clusters of other sizes.

In **icosahedral clusters**, each “k” layer consists of  $10k^2+2$  atoms.

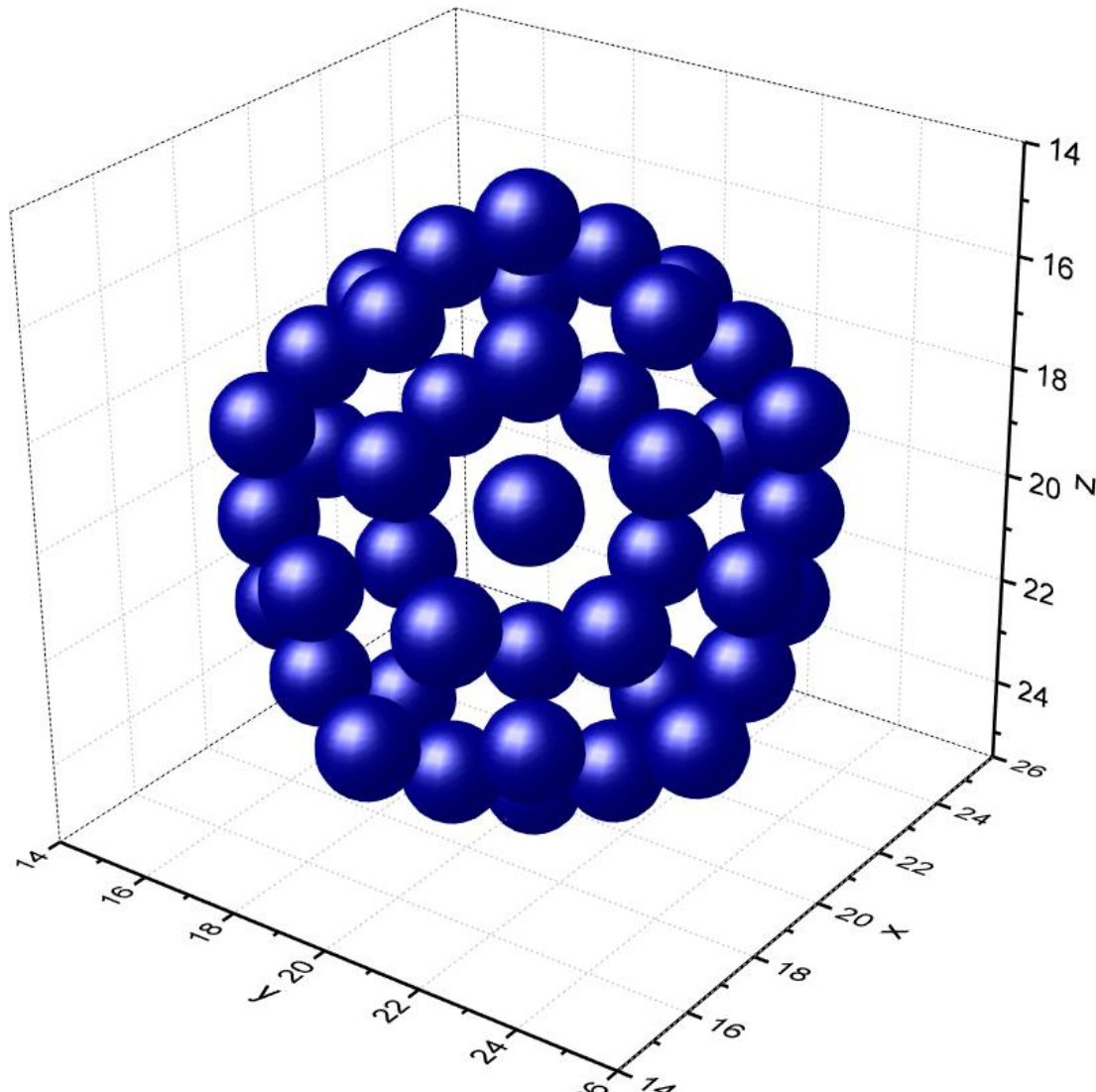
So the total number of atoms in a cluster with “N” layers is given by

$$n = (2N + 1) + 10 \sum_{k=1}^N k^2$$

$$n = 13, 55, 147, 309, 561 \quad \text{for } N=1, 2, 3, 4, 5$$

# Magic icosahedral cluster of 55 Pd atoms

Consider a cluster of 55 Pd atoms with **quasicrystalline** 5<sup>th</sup> order symmetry axis.



# Icosahedral cluster of 55 Pd atoms

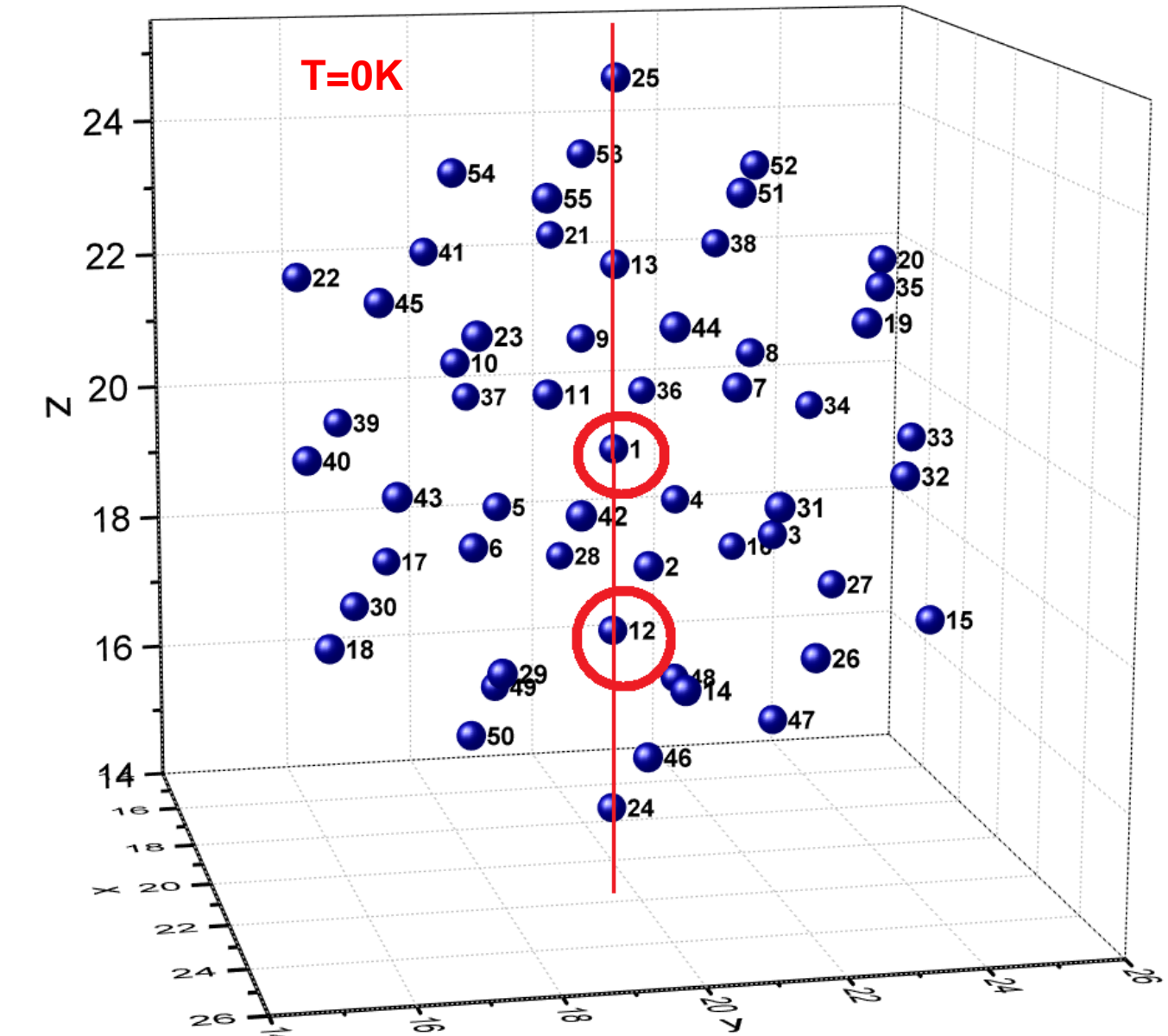
## Initial conditions:

at the initial time  
moment all  
particles have zero  
displacements  
from equilibrium  
positions.

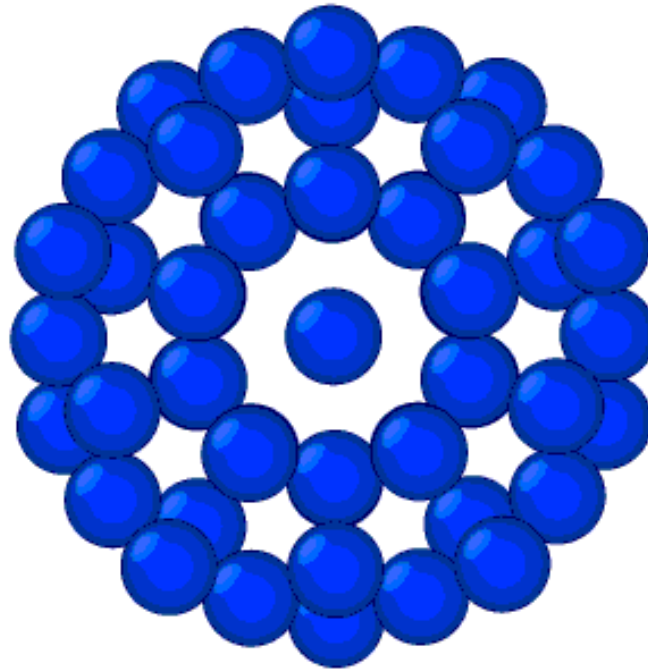
Atom #1 has initial  
kinetic energy  
**1.5eV** in [00-1]  
direction.

Atom #12 has  
initial kinetic  
energy **1.5eV** in  
[001] direction

**Boundary  
conditions:** free  
surfaces of cluster

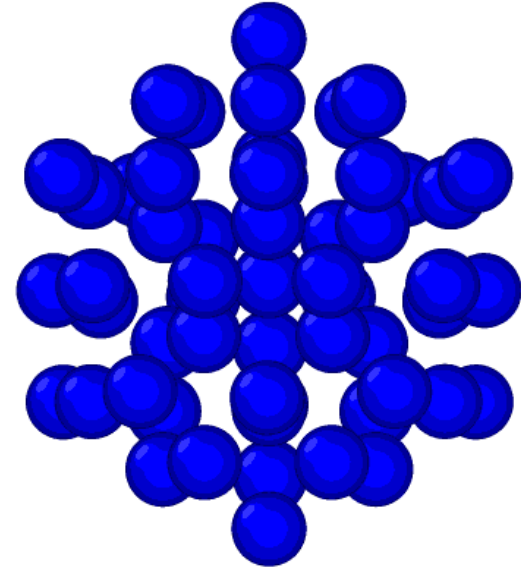
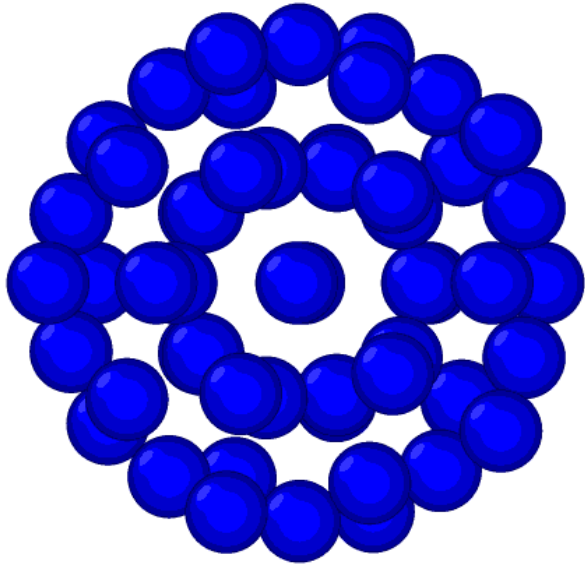


# Dynamics of the icosahedral cluster of 55 Pd atoms



It is seen from the visualization, that **Localized Anharmonic Vibration** is generated. The observed LAV in the atomic cluster represents the coherent collective oscillations of Pd atoms along quasi-crystalline symmetry directions.

# Dynamics of the Pd atomic cluster



If the initial energy, given to cluster is large enough (greater than the cohesive energy) then the cluster is destroyed after a certain period of time ( $\sim$  ps) .

# Conclusions and outlook

**New mechanism** of chemical and nuclear catalysis in solids is proposed, based on **time-periodic driving** of the potential landscape induced by *emerging nonlinear phenomena*, such as LAVs or phasons.

**The present mechanism** explains the salient LENR requirements: (i, ii) **long initiation time and high loading of D** within the Pd lattice as preconditioning needed to prepare small PdD crystals, in which DBs can be excited more easily, and (iii, iv) the **triggering by D flux or electric current**, which facilitates the DB creation by the input energy transformed into the lattice vibrations.

**The model** (*under selected set of material parameters*) describes **quantitatively** the observed **exponential dependence on temperature and linear dependence on the electric (or ion) current**.

Atomistic modeling of LAVs and phasons in metal hydrides/deuterides is an important outstanding problem since it may offer ways of ***engineering the nuclear active environment***.

# Publications

1. V.I. Dubinko, P.A. Selyshchev and F.R. Archilla, *Reaction-rate theory with account of the crystal anharmonicity*, **Phys. Rev. E** 83 (2011),041124-1-13
2. V.I. Dubinko, F. Piazza, *On the role of disorder in catalysis driven by discrete breathers*, **Letters on Materials** 4 (2014) 273-278.
3. V.I. Dubinko, *Low-energy Nuclear Reactions Driven by Discrete Breathers*, **J. Condensed Matter Nucl. Sci.**, 14, (2014) 87-107.
4. V.I. Dubinko, *Quantum tunneling in gap discrete breathers*, **Letters on Materials**, 5 (2015) 97-104.
5. V.I. Dubinko, *Quantum Tunneling in Breather ‘Nano-colliders’*, **J. Condensed Matter Nucl. Sci.**, 19, (2016) 1-12.
6. V. I. Dubinko, D. V. Laptev, *Chemical and nuclear catalysis driven by localized anharmonic vibrations*, **Letters on Materials** 6 (2016) 16–21.
7. V. I. Dubinko, *Radiation-induced catalysis of low energy nuclear reactions in solids*, **J. Micromechanics and Molecular Physics**, 1 (2016) 165006 -1-12.
8. V.I. Dubinko, O.M. Bovda, O.E. Dmitrenko, V.M. Borysenko, I.V. Kolodiy, *Peculiarities of hydrogen absorption by melt spun amorphous alloys  $Nd_{90}Fe_{10}$* , *Vestnik KhNU* (2016).
9. V. Dubinko, D. Laptev, K. Irwin, *Catalytic mechanism of LENR in quasicrystals based on localized anharmonic vibrations and phasons*, **ICCF20**, <https://arxiv.org/abs/1609.06625>.

## **Acknowledgments:**

- The authors would like to thank Dmitry Terentyev for his assistance in MD simulations
- Financial support from Quantum Gravity Research is gratefully acknowledged.



**THANK YOU  
FOR YOUR ATTENTION!**